Physics – Uspekhi **45** (1) 1 – 26 (2002)

REVIEWS OF TOPICAL PROBLEMS PACS numbers: **34.10.+x**, **34.70.+e**

Electron transitions in slow collisions of negative and positive atomic ions

M I Chibisov

DOI: 10.1070/PU2002v045n01ABEH001004

Contents

Abstract. Theoretical investigations of charge exchange and ionization processes accompanying collisions of negative and positive atomic ions are reviewed. Detailed analysis of the Coulomb Green function provides vast information about these processes. In particular, we took previously unknown sums of Coulomb wave function products over degenerate states. Adiabatic energies of the system and its wave functions can be expressed through these sums, whereas the wave functions turn out to possess very interesting and unexpected properties.

1. Introduction

Processes with the participation of negative ions have been scrutinized intensively in atomic collision physics. The attention was focused on the processes of ion recombination in collisions with positive ions:

$$A^- + B^{Z+} \to A + B^{(Z-1)+}(n)\,, \tag{1}$$

and ion production in the collisions of highly excited Rydberg atoms with atoms in ground states:

$$A + B^*(n) \to A^- + B^+\,. \tag{2}$$

Both small and large collision velocities were investigated. In the review we only consider slow collisions, i.e. those with the collision velocity $v < v_0 = 2.19 \times 10^8$ cm s^{-1}.

M I Chibisov Russian Research Centre 'Kurchatov Institute', Institute for Nuclear Fusion
pl. Kurchatova 1, 123182 Moscow, Russian Federation
Tel. (7-095) 196 70 41. Fax (7-095) 943 00 73
E-mail: chib@nfi.kiae.ru

Received 20 May, revised 17 September 2001
Uspekhi Fizicheskikh Nauk **172** (1) 3 – 29 (2002)
Translated by M I Chibisov; edited by A Radzig

Atomic negative ions constitute many-electron systems. The simplest such system with only two electrons is the hydrogen negative ion $H^-(1s^2)$. The binding energy of the weakly bound outer electron (or electron affinity of atomic hydrogen) is equal to 0.75421 eV. Electron affinities of many other atoms are smaller. Because of the minor electron affinity of atomic particles, the effective cross sections of processes (1) and (2) are rather large.

The perturbation of inner electrons in the atomic negative ion by the weakly bound outer electron is weak. Then one can rely on a one-electron approximation when describing processes (1) and (2). The neutral atom produces electric field with the potential V in which the weakly bound outer electron moves. This atomic electric potential is nonzero in the bounded volume. In the adiabatic approximation, the wave function of the outer electron in the system $A^- + B^{Z+}$, the function $\Phi(\mathbf{R}, \mathbf{r})$, is a solution of the steady-state wave equation where the vector $\mathbf{R}$ of internuclear distance is constant, i.e. this vector is an equation parameter. The wave equation has the following form

$$\left(-\frac{\Delta}{2} - \frac{Z}{r} + V\left(|\mathbf{R} - \mathbf{r}|\right) - E(R)\right)\Phi(\mathbf{R}, \mathbf{r}) = 0\,, \tag{3}$$

where $\mathbf{r}$ is the radius vector of the weakly bound electron, and $-Z/r$ is the Coulomb potential of the ion B^{Z+}. The coordinate origin is placed at the center of the Coulomb field, i.e. in the nucleus of the ion B^{Z+}. The electron energy $E(R)$ and wave function $\Phi(\mathbf{R}, \mathbf{r})$ depend on the absolute value of internuclear distance R and on the vector $\mathbf{R}$, respectively. Hartree atomic units ($e = m = \hbar = 1$) are used throughout this paper, unless stated otherwise.

Let us consider the Coulomb Green function $G(\mathbf{r}, \mathbf{r}', E)$. It is a solution of the following equation

$$\left(-\frac{\Delta}{2} - \frac{Z}{r} - E\right) G(\mathbf{r}, \mathbf{R}, E) = \delta(\mathbf{r} - \mathbf{R})\,. \tag{4}$$

The spectral representation of the Green function is given by

$$G(\mathbf{r},\mathbf{R},E)=\sum_{n,l,m}\frac{\psi_{nlm}(\mathbf{r})\,\psi^{*}_{nlm}(\mathbf{R})}{E_n-E}\,, \tag{5}$$

where $\psi_{nlm}(\mathbf{r})$ are the Coulomb spherical eigenfunctions. The sum in expression (5) represents both the summation over the discrete states with negative energies and integration over the continuum.

The exact solution of equation (4) and a compact expression for the Coulomb Green function was derived by Hostler and Pratt [1, 2] in 1963:

$$G(\mathbf{r},\mathbf{r}',E)=\frac{\Gamma(1-Z\nu)}{2\pi|\mathbf{r}-\mathbf{r}'|}\left[W(\tau_x)\,M'(\tau_y)-W'(\tau_x),M(\tau_y)\right], \tag{6}$$

$$\tau_{\{x,y\}}=\frac{\{x,y\}}{\nu}\,,\quad x=r+r'+|\mathbf{r}-\mathbf{r}'|\,,\quad y=r+r'-|\mathbf{r}-\mathbf{r}'|\,,\quad \nu\equiv\frac{1}{\sqrt{-2E}}\,. \tag{7}$$

Functions M and W are the Whittaker functions with indices $Z\nu$, 1/2 (viz. $M_{Z\nu,1/2}$, $W_{Z\nu,1/2}$). These functions are solutions of the equation

$$W''_{Z\nu,1/2}(\tau)+\left(-\frac{1}{4}+\frac{Z\nu}{\tau}\right)W_{Z\nu,1/2}(\tau)=0\,. \tag{8}$$

The function M is regular at the coordinate origin but is exponentially divergent as $\tau\to\infty$. The function W diminishes exponentially at infinity but is not regular at the origin.

Instead of differential equation (3) one can write down the following integral equation

$$\Phi(\mathbf{R},\mathbf{r})=-\int G(\mathbf{r},\mathbf{r}',E)\,V\big(|\mathbf{r}'-\mathbf{R}|\big)\,\Phi(\mathbf{R},\mathbf{r}')\,\mathrm{d}\mathbf{r}'\,. \tag{9}$$

The above equation is the main ingredient in the construction of the weakly bound electron wave function in the system A^-+B^{Z+}.

The interaction of the outer electron with the atomic core in a negative ion differs from zero only in a relatively small potential well volume. For example, the static potential well V of atomic hydrogen H($1s$) in the ground state is $V_{H(1s)}=\exp(-2r_A)(1+r_A^{-1})$, where $r_A\equiv|\mathbf{r}-\mathbf{R}|$. For large r_A, the polarization term $\alpha/2r_A^4$ should be added to this potential.

If the size of the potential well V is small, one can use a Taylor series expansion of the Green function in terms of the variable $\mathbf{r}'$ at the point $\mathbf{r}'=\mathbf{R}$ in equation (9):

$$G(\mathbf{r},\mathbf{r}',E)\approx G(\mathbf{r},\mathbf{R},E)+(\mathbf{r}'-\mathbf{R})\left.\frac{\mathrm{d}G}{\mathrm{d}\mathbf{r}'}\right|_{\mathbf{r}'=\mathbf{R}}+\ldots \tag{10}$$

At large internuclear distances R and in the vicinity of atom A, the wave function Φ is close to the unperturbed wave function Φ_0 of an isolated negative ion A^-. The latter can be substituted into the integral equation (9). Then, for zero angular momentum of negative ion, $L=0$, when Φ_0 does not depend on angles, the adiabatic wave function is proportional to the Green function at any point $\mathbf{r}$:

$$\Phi(\mathbf{R},\mathbf{r})\approx C_0G(\mathbf{r},\mathbf{R},E)\,,\qquad L=0\,, \tag{11}$$

where C_0 is the normalization constant. The total set of eigenfunctions of the systems A^-+B^{Z+} and $A+B^{(Z-1)}(n)$ can be derived by means of formula (11). For negative ions with $L\neq 0$, the eigenfunctions are proportional to derivatives of the Green function at $\mathbf{r}'=\mathbf{R}$.

Authors of early works [3–6] proceeded from the δ-model approach for the potential V of an atom A: $V=V_0\delta(\mathbf{r}-\mathbf{R})$. Energy levels of the system were derived in this approach by a numerical solution of a transcendental equation with the following logarithmic derivative of the Coulomb Green function: $\mathrm{d}\ln\big\{|\mathbf{r}-\mathbf{R}|\,G(\mathbf{r},\mathbf{R},E)\big\}/\mathrm{d}|\mathbf{r}-\mathbf{R}|$ at $\mathbf{r}=\mathbf{R}$. In the Landau–Zener approximation [7], the cross section of the recombination process (1) was calculated in paper [3] with the energy level splittings derived using δ-potential method. In paper [4], spectral line broadening and shifts were investigated using the same method. The δ-potential approach is applicable only for systems with zero orbital momentum of the negative ion ($L=0$). The results obtained by the δ-potential approach are discussed in more detail in book [6].

A detailed investigation of function (11) was carried out in papers [8–10]. The normalization integral was calculated on the plane $\{E,R\}$ where the energy E and internuclear distance R are independent variables, or where E and R are connected by the zero-order relation

$$E\approx E_0(R)=\varepsilon_0-\frac{Z}{R}\,, \tag{12}$$

which stems from the negative ion's attraction to the positive ion. Here ε_0 is the binding energy of an unperturbed negative ion. In these calculations the resonant behavior of the wave function normalization factor entering into Eqn (11) was revealed. Normalization factor resonances are placed at internuclear distances such that ionic term (12) crosses the Coulomb energy levels $E_n=-Z^2/2n^2$. In the vicinities of these crossings, the outer electron transfers from the negative ion to the positive one and then comes back.

In papers [8–10], the function $B(R)$ was introduced and investigated. The square of this function describes the admixture of the normalized negative ion wave function in the total adiabatic wave function (11). It was found that this function has zeros at the crossing points. The amplitude of the function between crossings is close to one. If the function $B(R)$ is equal to zero, then the outer electron is located near the positive ion B^{Z+} and the probability of finding the electron near the atom A is close to zero. On the contrary, if $B(R)\approx 1$, the outer electron resides near atom A, thus forming an ion A^-.

At large internuclear distances R, the potential barrier in the system A^-+B^{Z+} is located between atomic particles A and B^{Z+}. The probability of finding outer electron near the atom A or near the ion B^{Z+} depends on the quantum barrier penetrability. In this approach at large R and between crossing points the probability of finding an electron near the positive ion should be small [or function $B(R)$ should be close to unity: $B(R)\simeq 1$]. However, the absolute value of the difference $|1-B(R)|$ in the barrier factor approach is much larger than that found in the calculations [8–10].

In reality, in the Coulomb field of the ion B^{Z+} the negative energy states do not form a continuous spectrum of states. The wave function behavior is controlled by the regularity condition at the Coulomb center. As a consequence of this condition, the amplitude of the wave function (11) in the neighborhood of the positive ion B^{Z+} is, in ranges between energy level crossings, appreciably smaller than that resulting

from the barrier penetrability estimation. Accordingly, the value of the function $B(R)$ appears to be very close to one. The graphs of the function $B(R)$ and normalization constant are presented below.

A Coulomb system possesses four-dimensional symmetry and the degeneracy of the Coulomb energy levels is a consequence of this property. Because of the energy level degeneracy, the Coulomb Green function (6) and the adiabatic wave function (11) depend on the sums of the Coulomb wave function products over orbital quantum numbers l, m with the same principal quantum number n, namely $\sum_{l,m} \psi^*_{nlm}(\mathbf{r})\,\psi_{nlm}(\mathbf{R})$. These functions correspond to the states with the same energy $E_n = -Z^2/2n^2$. For negative ions with a nonzero angular momentum, the adiabatic wave functions depend on the sums of the products of the Coulomb wave functions and their derivatives.

The sums of the Coulomb wave function products have been calculated and investigated in papers [8, 11–13]. It was found that these sums are expressed in terms of the quadratic form that depends on the wave function of only one state, namely, on the function ψ_{n00} with zero orbital momentum $l = m = 0$. In these quadratic forms, the functions ψ_{n00} depend on the two-center elliptic coordinates $\xi, \eta = (r \pm |\mathbf{r} - \mathbf{R}|)/R$. The sums of interest were obtained by investigating the limiting behavior of the Coulomb Green function (6) as the energy E approached the Coulomb energy level E_n. This limit was then compared with the appropriate limit of the spectral representation (5) of the Green function. These sums were not known before. In 1935, V A Fock calculated a similar sum for wave functions in momentum representation.

The possibility of expressing adiabatic wave functions (11) through the functions $\psi_{n00}(\xi)$ and $\psi_{n00}(\eta)$ greatly simplifies the investigation of these wave functions. It has been found that in the states governed by the adiabatic wave functions (11) the electron has a dipole moment that depends on the internuclear distance R. At infinitely large internuclear distances ($R \to \infty$), the limits of functions (11) are the wave functions of Stark states, i.e. functions (11) transform to the wave functions in parabolic coordinates [7]. The limits of dipole moments are $-3n(n_1 - n_2)/2Z$ that are dipole moments of the Stark states [7].

It is well known that Stark states are the Coulomb eigenstates in a weak uniform electric field [7]. It was found that Stark states are also formed when the Coulomb Rydberg states are perturbed by a neutral atom in the limit $R > r_n$, where $r_n = 2n^2/Z$ is the size of the Rydberg orbit. This result is very important for investigations of laser radiation interaction with Rydberg atoms in a gas medium of neutral atoms.

Normalization factors of adiabatic wave functions (11) depend on the above-discussed sums with $\mathbf{r} = \mathbf{R}$. Many such sums were calculated in papers [8, 11–13]. They exhibit a specific behavior as the functions of internuclear distance R. Energy splittings at avoided crossings of ionic and covalent electronic terms are expressed through the sums [8] that do not have zeros at finite values of R and decay exponentially as $R \to \infty$. As a result, all the electronic energy crossings in the system $A^- + B^{Z+}$ are really avoided crossings but not strict crossings.

It has been found in earlier works [3–6] that in the δ-potential approach the ionic term couples with only one covalent term from n^2 degenerate states with the same principal quantum number n. This covalent state was referred to as the 'active' state. The wave functions of the active states are given by formula (11). The energies of these states depend on R. The remaining $n^2 - 1$ states are passive and do not interact with the ionic state; the energies of these states are independent of R and all equal to the Coulomb energy E_n.

The basis of n^2 degenerate Coulomb states can be reconstructed by introducing the linear combinations of Coulomb wave functions $\psi_{nlm}(\mathbf{r})$ for every n. Wave function (11) is one of these combinations, and the wave functions of passive states represent the other $n^2 - 1$ combinations. Because the wave functions of passive states are orthogonal to function (11), they depend on R and are closely coupled with the active state in the time-dependent Schrödinger equation. Thus, passive states are occupied in collisions (1) and (2), which increases appropriate cross sections. If that is the case, the passive states are not in reality passive. In paper [8], the complete basis set of n^2 orthonormal wave functions was constructed for every n.

Adiabatic wave functions (11) have not been studied previously. In calculating the cross section of recombination process (1) it was not possible to get the populations of individual states because the adiabatic wave functions (11) differ essentially from the Coulomb spherical functions $\psi_{nlm}(\mathbf{r})$ [3]. The calculation of the cross section of the inverse process (2) and investigations of spectral line broadening and shifts are not possible in this approach at all, because of the problem of initial states [14].

The collisions of two negative ions discussed below can be described, generally speaking, by means of the Green function for the Coulomb field of repulsion. However, the one-electron approach is not applicable to the system $A^- + B^-$ because both weakly bound electrons can be detached in this collision. At large internuclear distances, the wave function of every weakly bound electron can be expressed through the appropriate Green function. The total wave function is equal to the product of these Green functions, which complicates the analysis. On the other hand, in the repulsion field there are no excited Rydberg states and this simplifies the problem. The total set of ionized states consists of two states evolving through the one-electron ionization channels $A^- + B + e$ and $A + e + B^-$, and of one state attendant to two-electron detachment channel $A + B + 2e$. The probabilities of passing all channels are determined by the Coulomb repulsion of weakly bound electrons and are in strong competition. All these channels should be incorporated in a system of closely coupled equations. If the electron of the ion A^- is detached then the system $A + B^-$ is formed and the subsequent electron detachment from the ion B^- is only possible as a result of the weaker interaction with the neutral atom A.

A more detailed analysis of the problems related to the collisions of negative and positive atomic ions is given below.

2. Adiabatic states of the system $A^- + B^{Z+}$

2.1 Negative ions with zero orbital momenta

The wave function of the outer electron in the unperturbed negative ion with an orbital momentum $L = 0$ can be written in the form

$$\Phi_0(|\mathbf{r} - \mathbf{R}|) = N_0 \frac{\exp(-\gamma|\mathbf{r} - \mathbf{R}|)}{|\mathbf{r} - \mathbf{R}|}, \qquad (13)$$

$$N_0 = \sqrt{\frac{\gamma}{2\pi}}, \qquad \varepsilon_0 = -\frac{\gamma^2}{2}, \qquad L = 0$$

that is the limit of the wave function Φ of the ionic state at infinite internuclear separation ($R \to \infty$). Let us investigate in more details the relationship between the unperturbed wave function (13) and the Coulomb Green function which, in accordance with formula (11), is the wave function of the outer electron of the negative ion in the presence of a positive ion.

The Whittaker function M is defined as the linear combination of functions $W_-(\tau)$ and $W_+(\tau)$ [84]:

$$\Gamma(1-Zv)\,M_{Zv,1/2}(\tau) = (-1)^{1+Zv}\,\frac{\Gamma(1-Zv)}{\Gamma(1+Zv)}\,W_-(\tau) + (-1)^{Zv}\,W_+(\tau)\,, \tag{14}$$

where the function $W_-(\tau) \equiv W_{Zv,1/2}(\tau)$ is exponentially decreasing and the function $W_+(\tau) \equiv W_{-Zv,1/2}(-\tau)$ is exponentially increasing for large arguments $\tau \to \infty$. Using this linear combination we can write out the Green function (6) at $\mathbf{r}' = \mathbf{R}$ as the sum of two terms:

$$G(\mathbf{r},\mathbf{R},E) = \frac{(-1)^{1+Zv}}{2\pi}\,\frac{\Gamma(1-Zv)}{\Gamma(1+Zv)}\,G_1(\mathbf{r},\mathbf{R},E) + \frac{(-1)^{Zv}}{2\pi}\,G_2(\mathbf{r},\mathbf{R},E)\,, \tag{15}$$

where

$$G_1(\mathbf{r},\mathbf{R},E) = \frac{W_-(\tau_x)\,W'_-(\tau_y) - W'_-(\tau_x)\,W_-(\tau_y)}{|\mathbf{r}-\mathbf{R}|}\,, \tag{16}$$

$$G_2(\mathbf{r},\mathbf{R},E) = \frac{W_-(\tau_x)\,W'_+(\tau_y) - W'_-(\tau_x)\,W_+(\tau_y)}{|\mathbf{r}-\mathbf{R}|}\,. \tag{17}$$

The functions W_+ and W_- are not regular at the coordinate origin (at the Coulomb center) but their linear combination (14), i.e. the function M, is regular there. Accordingly, the functions G_1 and G_2 are not regular at the Coulomb center but their linear combination, i.e. the total Green function (15), is regular. The function G_2 can be called the ionic part of the Coulomb Green function, and the function G_1 the covalent part. The coefficients in the linear combination (15) are determined by the regularity condition at the Coulomb center. The properties of the system $A^- + B^{Z+}$ depend essentially on this condition.

The arguments τ_x, τ_y of the functions G_1 and G_2 are given by formulas (7). At fixed $\mathbf{r}' = \mathbf{R}$, these variables are proportional to the elliptic coordinates ξ, η [15]:

$$\tau_x = \frac{R}{v}(\xi+1)\,, \quad \tau_y = \frac{R}{v}(\eta+1)\,, \quad \xi,\eta = \frac{r \pm |\mathbf{R}-\mathbf{r}|}{R}\,,$$
$$1 \leqslant \xi \leqslant \infty\,, \quad -1 \leqslant \eta \leqslant +1\,.$$

Being exponentially divergent at large arguments, the function $M(\tau_y)$ depends on the variable τ_y which varies in the limits $0 \leqslant \tau_y \leqslant 2R/v$ and does not tend to infinity as $r \to \infty$. Therefore, functions G_1 and G_2 and the wave function (11) are regular as $r \to \infty$. The variable τ_x is varied in the limits $2R/v \leqslant \tau_x \leqslant \infty$, so that the irregularity of functions $W_\pm(\tau_x)$ does not manifest itself, because at finite values of R the variable τ_x is not equal to zero.

Let us investigate now the passage to the limit $\mathbf{r} \to \mathbf{R}$. The binding energies ε_0 of negative ions are small and the energies E_n of covalent states of the system $A + B^{(Z-1)+}(n)$, occupied in collision (1), are also small. For small energies we can avail ourselves of the asymptotics of the Whittaker functions in the index $Zv \to \infty$ [16] or calculate them in the semiclassical approach invoked for solving equation (8). We shall rely on the semiclassical approach and then the solutions of equation (8) in the subbarrier region are given by [9]

$$W_\pm(\tau) = \left(1-\frac{\tau_0}{\tau}\right)^{-1/4} \exp\left[\pm\frac{1}{2}\sqrt{\tau(\tau-\tau_0)} \pm Zv \pm 2Zv\,\ln\frac{\sqrt{\tau}-\sqrt{\tau-\tau_0}}{2Zv}\right]. \tag{18}$$

The function M is expressed as the linear combination (14) of functions (18).

A semiclassical representation (18) is conveniently used for investigating the ionic part G_2 of the Green function in the region close to a negative ion. Expanding G_2 at $|\mathbf{r}-\mathbf{R}| \ll R$ we obtain

$$G_2(\mathbf{r},\mathbf{R},E) \approx \frac{\exp\left(-\gamma_{\rm scl}|\mathbf{r}-\mathbf{R}|\right)}{|\mathbf{r}-\mathbf{R}|}\,,$$
$$\gamma_{\rm scl}(R) \equiv \left[-2\left(E+\frac{Z}{R}\right)\right]^{1/2}. \tag{19}$$

The form of function (19) is the same as the form of the unperturbed function (13). If the energy E is equal to the negative ion energy in the zero approximation (12), then the exponential powers coincide as well: $\gamma_{\rm scl} = \gamma$. Numerical calculations with the use of exact Whittaker functions, carried out by us, have shown that expression (19) coincides with the results of numerical calculations in the subbarrier region with a high accuracy for $Zv \geqslant 2$.

The function G_1 is regular as $\mathbf{r} \to \mathbf{R}$, and in the vicinity of the negative ion the expansion of this function assumes the form

$$G_1(\mathbf{r},\mathbf{R},E) = \frac{W_+(\tau_x)\,W'_+(\tau_y) - W'_+(\tau_x)\,W_+(\tau_y)}{|\mathbf{r}-\mathbf{R}|} \approx \frac{v}{2}\left[\left(\frac{\mathrm{d}W_+}{\mathrm{d}R}\right)^2 + 2\left(E+\frac{Z}{R}\right)W_+^2\right]_{\tau=2R/v} - \frac{Zv}{2}(r-R)\,\frac{W_+^2(2R/v)}{R^2} + \ldots \tag{20}$$

We now turn our attention to the normalization of the Green function regarded as a wave function in accordance with relation (11). The normalized wave function $\Phi(\mathbf{R},\mathbf{r})$ can be written in the form

$$\Phi(\mathbf{R},\mathbf{r}) = \frac{N(R)}{|\mathbf{r}-\mathbf{R}|}\left[W\left(\frac{x}{v}\right)M'\left(\frac{y}{v}\right) - W'\left(\frac{x}{v}\right)M\left(\frac{y}{v}\right)\right], \tag{21}$$

where the normalization factor

$$N(R) = \left\{\int \mathrm{d}\tau_x\,\mathrm{d}\tau_y\,\frac{1}{(\mathbf{r}-\mathbf{R})^2} \times\left[W\left(\frac{x}{v}\right)M'\left(\frac{y}{v}\right) - W'\left(\frac{x}{v}\right)M\left(\frac{y}{v}\right)\right]^2\right\}^{-1/2}, \tag{22}$$

or in the form

$$\Phi(\mathbf{R},\mathbf{r}) = 2\pi N_0\,B(R)\,G(\mathbf{r},\mathbf{R},E) = N(R)\,\frac{G_1(\mathbf{r},\mathbf{R},E)}{\Gamma(1+Zv)} + N_0\,B(R)\,G_2(\mathbf{r},\mathbf{R},E)\,, \tag{23}$$

where the function $B(R)$ is defined in the following way

$$B(R) \equiv \frac{N(R)}{N_0 \Gamma(1 - Zv)} \,. \tag{24}$$

The normalization factor $N(R)$ has been calculated numerically [9, 10] on the basis of the series representation of Whittaker functions W and M over positive degrees of an argument [84]. The adiabatic energy of the system as a function of the internuclear distance R was taken in zero approximation (12). The derived function $N(R)$ is shown in Fig. 1. As illustrated, $N(R)$ passes through sharp maximums located at term crossing positions where $E(R) = E_n = -Z^2/2n^2$, from which R_n can be calculated in the zero approximation for the ionic energy (12):

$$E_n = \varepsilon_0 - \frac{Z}{R_n} \,, \qquad R_n = \frac{Z}{\varepsilon_0 - E_n} \,. \tag{25}$$

Far from the term crossings ($R_n < R < R_{n+1}$), the exponentially increasing term in the linear combination (14) is the leading one. In this case integrand in Eqn (22) is large and the normalization factor $N(R)$ is small. Alternatively, near crossings ($R \approx R_n$), the exponentially decreasing term is dominant in the linear combination (14); the integrand in Eqn (22) is small and $N(R)$ has a maximum.

In Fig. 2, the calculated function $B(R)$ is depicted. Far from crossings, the $B(R)$ function is close to 1. The equality of the function $B(R)$ to unity signifies that the outer electron is located near the negative ion [see formula (23)]. Indeed, the first term with the function G_2 in the normalized Green function [see formulas (15), (23)] is small in this case, and the second term with G_1 coincides with the unperturbed function (13). The second terms in Eqns (15) and (23) are given by expression (19) at all distances R. In the zero approximation for the energy (12), when $\gamma_{\rm scl} = \gamma$, the second terms in expressions (15), (23) and hence the complete ionic function $\Phi(\mathbf{R}, \mathbf{r})$ are close to the unperturbed function (13) and the electron spends more time near the negative ion. At crossings, when the exponentially decreasing term in Eqn (14) is the leading one, the function $B(R)$ drops to zero and the electron leaves its position for a positive ion. In formula (15), the first term containing G_2 becomes the leading one.

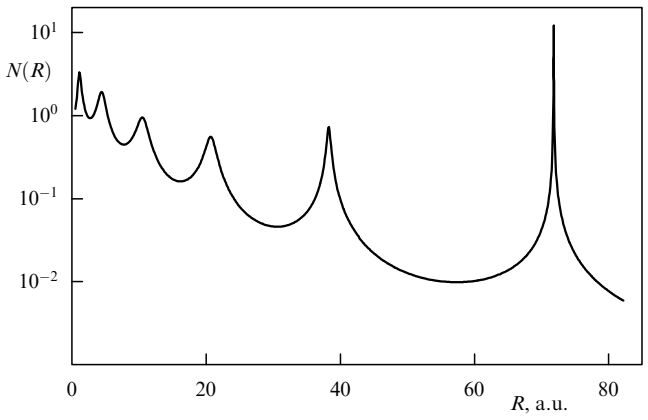

Figure 1. Normalization factor $N(R)$ as a function of internuclear distance R for the colliding system $H^- + He^{++}$.

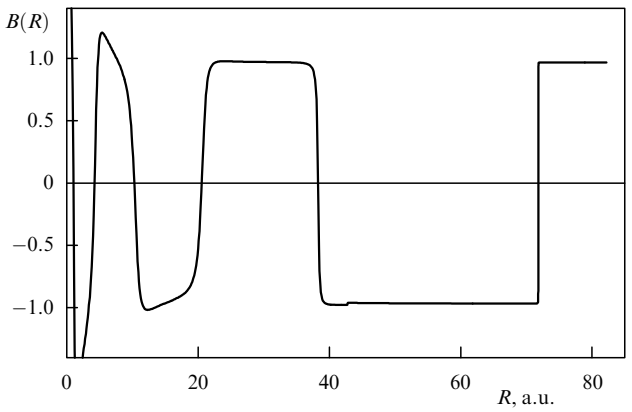

Figure 2. Function $B(R)$ versus internuclear distance R for the colliding system $H^- + He^{++}$.

Using the spectral representation (5) of the Green function we can write out an analogous representation for the adiabatic wave function (11):

$$\Phi(\mathbf{R}, \mathbf{r}) = \sum_n C_n(E)\, \Psi_n(\mathbf{R}, \mathbf{r}) \,, \tag{26}$$

where the normalized adiabatic wave functions $\Psi_n(\mathbf{R}, \mathbf{r})$ of covalent states are defined by the sums of the Coulomb wave function products:

$$\Psi_n(\mathbf{R}, \mathbf{r}) = \sum_{l=0}^{n-1} \sum_{m=-l}^{l} J_{nlm}(\mathbf{R})\, \psi^*_{nlm}(\mathbf{r}) \,, \tag{27}$$

$$J_{nlm}(\mathbf{R}) \equiv \frac{\psi_{nlm}(\mathbf{R})}{\sqrt{Q_n(R)}} = \int \psi_{nlm}(\mathbf{r})\, \Psi_n(\mathbf{R}, \mathbf{r})\, \mathrm{d}\mathbf{r} \,, \tag{28}$$

and the coefficients $C_n(R)$ and the sum $Q_n(R)$ are equal to

$$C_n(R) = -\frac{2\pi N_0 B(R)}{E - E_n}\, Q_n^{1/2}(R) \,, \tag{29}$$

$$Q_n(R) \equiv \sum_{l=0}^{n-1} \sum_{m=-l}^{l} \left|\psi_{nlm}(\mathbf{R})\right|^2 . \tag{30}$$

If the energy E coincides with the Coulomb eigenenergy ($E = E_n$), then the denominator in formula (29) becomes zero. However, the coefficient $C_n(R)$ remains finite because at this energy the function $B(R)$ is also equal to zero (see above).

So, in the approximation being considered the wave functions of adiabatic states are constructed from the functions $\Psi_n(\mathbf{R}, \mathbf{r})$ which are sums of the Coulomb wave function products over degenerate states. The basis of n^2 degenerate states can be reconstructed [6, 17] by the use of linear combinations made up from the initial wave functions. For every principal quantum number n, only one state (in more exact terms only one combination of degenerate states) is present in the expansion (26). All the other $n^2 - 1$ passive states are not present in the expansion (26). The complete orthonormal basis of adiabatic wave functions is constructed below.

Coulomb eigenfunctions written in the spherical coordinates, viz. $\psi_{nlm}(\mathbf{r}) = N_{nl} f_{nl}(r)\, Y_{lm}(\theta, \phi)$, depend on the z-axis direction of the coordinate system because the spherical harmonics $Y_{lm}(\theta, \phi)$ are transformed when the coordinate z-axis rotates [18]. Using the addition theorem for spherical harmonics [7, 18]:

$$\sum_{m=-l}^{l} Y^*_{lm}(\theta, \phi)\, Y_{lm}(\theta_R, \phi_R) = \frac{2l+1}{4\pi}\, P_l(\cos\alpha) \,, \tag{31}$$

where θ_R and ϕ_R are the spherical angles of the vector $\mathbf{R}$, and α is the angle between vectors $\mathbf{r}$ and $\mathbf{R}$, we can write down the wave functions $\Psi_n(\mathbf{R},\mathbf{r})$ of active states and the sums $Q_n(R)$ in the form of single sums over an orbital momentum l only:

$$\Psi_n(\mathbf{R},\mathbf{r}) = \frac{1}{\sqrt{Q_n(R)}} \sum_{l=0}^{n-1} \frac{2l+1}{4\pi} P_l(\cos\alpha) f_{nl}(r) f_{nl}(R)\,, \quad (32)$$

$$Q_n(R) = \sum_{l=0}^{n-1} \frac{2l+1}{4\pi} \left|f_{nl}(R)\right|^2 . \quad (33)$$

Expressions (32) and (33) for $Q_n(R)$ and $\Psi_n(\mathbf{R},\mathbf{r})$ do not depend on the z-axis direction in the reference system and can be calculated in an arbitrary oriented coordinate system. The subsequent summation in these expressions over l is carried out in a closed form making use of the Hostler – Pratt Green function (6) (see below).

2.2 Negative ion with an orbital momentum $L = 1$

The three angular components $\{x, y, z\}$ of the unperturbed wave function of the weakly bound electron with an orbital momentum $L = 1$ can be written out in the form

$$\Phi_{0,\{x,y,z\}}(\mathbf{r}_b) = \sqrt{\frac{3}{4\pi}} \frac{\chi_0(r_b)}{r_b} \times \{\cos\theta_b, \sin\theta_b\cos\phi_b, \sin\theta_b\sin\phi_b\}, \quad \mathbf{r}_b = \mathbf{r} - \mathbf{R}\,, \quad (34)$$

where the radial function $\chi_0(r_b)$ is the solution of the equation

$$\frac{\mathrm{d}^2\chi_0(r_b)}{\mathrm{d}r_b^2} + \left[2\big(\varepsilon_0 - V(r_b)\big) - \frac{L(L+1)}{r_b^2}\right]\chi_0(r_b) = 0\,, \quad L = 1\,. \quad (35)$$

Substituting the wave function (34) and the expansion of the Green function (10) into the right-hand part of the integral equation (9), we obtain that the integral (9) of the first term in the expansion (10) is equal to zero.

For a negative ion with an orbital momentum $L = 1$, the adiabatic two-center wave function of the outer electron is given by the second term in the expansion (10) and is therefore proportional to the derivatives of the Green function:

$$\Phi_z = -\cos\theta_b\, N_z \frac{F_z\{M,W\}}{|\mathbf{r}-\mathbf{R}|} \approx \left.\frac{\partial G}{\partial z'}\right|_{\mathbf{r}'\to\mathbf{R}}, \quad (36)$$

$$\Phi_x = -\sin\theta_b\cos\varphi_b N_x \frac{F_x\{M,W\}}{|\mathbf{r}-\mathbf{R}|} \approx \left.\frac{\partial G}{\partial x'}\right|_{\mathbf{r}'\to\mathbf{R}}, \quad (37)$$

$$\Phi_y = -\sin\theta_b\sin\varphi_b\, N_y \frac{F_y\{M,W\}}{|\mathbf{r}-\mathbf{R}|} \approx \left.\frac{\partial G}{\partial y'}\right|_{\mathbf{r}'\to\mathbf{R}}, \quad (38)$$

where θ_b and φ_b are the spherical angles of the vector $\mathbf{r}_b \equiv \mathbf{r} - \mathbf{R}$ in the coordinate system the origin of which is placed in the nucleus of the negative ion, and $N_{x,y,z}$ are the normalization factors. If the z-axis is directed along the vector $\mathbf{R}$, then one finds

$$F_z\{M,W\} \equiv \frac{2}{v} W'M' + \left(-\frac{1}{2v} + \frac{Zv}{R}\frac{R-r}{R-z}\right) WM - \frac{WM' - W'M}{|\mathbf{R}-\mathbf{r}|}\,, \quad (39)$$

$$F_{x,y}\{M,W\} \equiv \frac{2}{v} W'M' + \left(-\frac{1}{2v} + \frac{Zv}{R}\frac{r+R}{r+z}\right) WM - \frac{WM' - W'M}{|\mathbf{R}-\mathbf{r}|}\,, \quad (40)$$

where $F_x\{M,W\} = F_y\{M,W\} = F_{x,y}\{M,W\}$, and x, y, z are the components of the vector $\mathbf{r}$.

The asymptotics of the unperturbed radial function $\chi_0(r_b)$ entering into Eqn (35) is controlled mainly by the centrifugal potential. The atomic potential $V(r_b)$, which is determined at large distances by the polarization interaction $V(r_b) \to -\alpha/2r_b^4$, may be neglected. The asymptotics of $\chi_0(r_b)$ is then given by

$$\chi_0^{\mathrm{as}} = N_0^{(1)}\left(1 + \frac{1}{\gamma r_b}\right)\exp(-\gamma r_b)\,. \quad (41)$$

This expression is an exact solution of Eqn (35) for $V(r_b) \equiv 0$. The coefficient $N_0^{(1)} = 0.112$ for the ion Ca^- ($\varepsilon_0^{3/2} = 0.01973$ eV, $\varepsilon_0^{1/2} = 0.02455$ eV) was found by numerical solution of Eqn (35) with the model potential $V(r_b)$ in papers [19, 20].

Substituting the semiclassical expression (18) for Whittaker functions into formulas (39) and (40) and expanding them with the constraint $|\mathbf{r}-\mathbf{R}| \ll R$, we obtain

$$F_z \approx F_{x,y} \approx \left(1 + \frac{1}{\gamma_{\mathrm{scl}}|\mathbf{r}-\mathbf{R}|}\right)\exp\left(-\gamma_{\mathrm{scl}}|\mathbf{r}-\mathbf{R}|\right). \quad (42)$$

Here, the constant γ_{scl} is defined by Eqn (19) in the semiclassical approximation. Expression (42), to within a constant factor, coincides with the asymptotics (41) if the ionic-state energy is described in the zero-order approximation (12), when $\gamma_{\mathrm{scl}} = \gamma$. Thus, the constructed functions (36) – (38) satisfy the necessary condition: at large internuclear distances, they coincide with the unperturbed functions in the vicinity of the negative ion.

The main contribution to the normalization integral is made by the region of large distances from the negative ion nucleus, but the contribution from asymptotics (41) is divergent as $r_b \to 0$. Therefore, expressions (36) – (38) were matched with the numerical solution of equation (35). For the ion Ca^-, the behavior of quantities $N(R)$ and $B(R)$ as functions of the internuclear distance R for zero approximation to the ionic energy (12) is similar to the behavior of the same quantities for the system $H^- + He^{++}$, shown in Figs 1 and 2. In the case of the Ca^- ion, the number of energy levels crossed by the ionic term is larger because the electron binding energy of this ion is smaller.

For the case of the negative ion with an orbital momentum $L = 1$, the adiabatic wave functions are expressed in the following way:

$$\Phi_{x,y,z}(\mathbf{R},\mathbf{r}) = N_0^{(1)} \frac{\sqrt{3\pi}}{\gamma} B_{x,y,z}(E) \left.\frac{\partial G(\mathbf{r},\mathbf{r}',E)}{\partial\{x',y',z'\}}\right|_{\mathbf{r}'=\mathbf{R}}, \quad (43)$$

$$B_{x,y,z}(E) \equiv \frac{\gamma N_{x,y,z}(E)}{N_0^{(1)}\sqrt{3/4\pi}\,\Gamma(1-Zv)}\,. \quad (44)$$

With the use of the spectral representation of the Green function (5), we write down a similar expansion of adiabatic functions:

$$\Phi_{x,y,z}(\mathbf{R},\mathbf{r}) = \sum_n C_n^{x,y,z}(E)\,\Psi_n^{x,y,z}(\mathbf{R},\mathbf{r})\,, \quad (45)$$

where the normalized wave functions of covalent states are

$$\Psi_n^{x,y,z}(\mathbf{R},\mathbf{r}) = \frac{1}{\sqrt{Q_n^{x,y,z}(R)}} \sum_{l,m} \psi_{nlm}^*(\mathbf{r})\, \frac{\partial \psi_{nlm}(\mathbf{R})}{\partial\{x,y,z\}}\,. \qquad (46)$$

These functions are linear combinations of Coulomb spherical wave functions $\psi_{nlm}(\mathbf{r})$ with the common principal quantum number n and, consequently, with the equal energy.

The expansion coefficients and the normalization factors are defined as

$$C_n^{x,y,z}(E) = -\frac{N_0^{(1)}\sqrt{3\pi}}{\gamma}\, \frac{B_{x,y,z}(E)\,\sqrt{Q_n^{x,y,z}(R)}}{E_n - E}\,, \qquad (47)$$

$$Q_n^z(R) \equiv \sum_{l,m} \left| \frac{\partial \psi_{nlm}(\mathbf{R})}{\partial z} \right|^2_{z=R} = \sum_{l,m} \left| \frac{\partial \psi_{nlm}(\mathbf{R})}{\partial R} \right|^2, \qquad (48)$$

$$Q_n^{x,y}(R) \equiv \sum_{l,m} \left| \frac{\partial \psi_{nlm}(\mathbf{R})}{\partial\{x,y\}} \right|^2_{x=y=0} = \frac{1}{R^2} \sum_{l,m} \left| \frac{\partial \psi_{nlm}(\mathbf{R})}{\partial \theta} \right|^2_{\theta=0},$$

where two last sums with the indices x and y are the same.

When constructing the complete adiabatic basis set (see Section 2.3), the wave functions (46) should be expressed through the sums of the Coulomb functions ψ_{nlm} in a coordinate system the z'-axis of which is perpendicular to the collision plane. The x'-axis should be directed at a time either along the impact parameter (rectilinear trajectories) or along the vector of a closest approach (Coulomb trajectories, the point in time $t = 0$). This coordinate system x', y', z' is not rotated at collision.

If we pass on to a new coordinate system, then use could be made of the fact that the sum $\sum_{l,m} \psi_{nlm}^*(\mathbf{r})\, \psi_{nlm}(\mathbf{R})$ does not depend on the coordinate system orientation (see above). Because the derivatives in formula (48) are concerned with the vector $\mathbf{R}$, we should only redetermine these derivatives in the new coordinate system. Since the x-axis of the above-used rotating coordinate system coincides with the z-axis of the new nonrotating system, we have

$$\frac{\mathrm{d}}{\mathrm{d}x} = \frac{\mathrm{d}}{\mathrm{d}z'}\,,$$

$$\frac{\mathrm{d}}{\mathrm{d}z} = \cos\phi_R\, \frac{\mathrm{d}}{\mathrm{d}x'} + \sin\phi_R\, \frac{\mathrm{d}}{\mathrm{d}y'}\,,$$

$$\frac{\mathrm{d}}{\mathrm{d}y} = -\sin\phi_R\, \frac{\mathrm{d}}{\mathrm{d}x'} + \cos\phi_R\, \frac{\mathrm{d}}{\mathrm{d}y'}\,.$$

Transforming the derivatives with respect to x', y' to derivatives with respect to spherical coordinates R, θ, ϕ, we obtain the functions $\Psi_n^{x,y,z}(\mathbf{R},\mathbf{r})$ in the new nonrotating coordinate system:

$$\Psi_n^x(\mathbf{R},\mathbf{r}) = \sum_{l,m} \psi_{nlm}^*(\mathbf{r})\, J_{nlm}^x(\mathbf{R})\,, \quad J_{nlm}^x(\mathbf{R}) \equiv \frac{\partial \psi_{nlm}(\mathbf{R})/\partial\theta_R}{R\sqrt{Q_n^x(R)}}\,,$$

$$\Psi_n^y(\mathbf{R},\mathbf{r}) = \sum_{l,m} \psi_{nlm}^*(\mathbf{r})\, J_{nlm}^y(\mathbf{R})\,, \quad J_{nlm}^y(\mathbf{R}) \equiv \frac{\partial \psi_{nlm}(\mathbf{R})/\partial\phi_R}{R\sqrt{Q_n^y(R)}}\,,$$

$$\Psi_n^z(\mathbf{R},\mathbf{r}) = \sum_{l,m} \psi_{nlm}^*(\mathbf{r})\, J_{nlm}^z(\mathbf{R}), \quad J_{nlm}^z(\mathbf{R}) \equiv \frac{\partial \psi_{nlm}(\mathbf{R})/\partial R}{\sqrt{Q_n^z(R)}}\,, \qquad (49)$$

where θ_R and ϕ_R are the spherical angles of the vector $\mathbf{R}$. The polar angle θ_R is constant and equal to $\pi/2$ during the collision, because the z'-axis is perpendicular to the collision plane. The normalization factors $Q_n^{x,y,z}(R)$ are defined as

$$Q_n^x(R) = \frac{1}{R^2} \sum_{l,m} \left| \frac{\partial \psi_{nlm}(\mathbf{R})}{\partial \theta_R} \right|^2,$$

$$Q_n^y(R) = \frac{1}{R^2} \sum_{l,m} \left| \frac{\partial \psi_{nlm}(\mathbf{R})}{\partial \phi_R} \right|^2 = \frac{1}{R^2} \sum_{l,m} m^2 \left| \psi_{nlm}(\mathbf{R}) \right|^2, \qquad (50)$$

$$Q_n^z(R) = \sum_{l,m} \left| \frac{\partial \psi_{nlm}(\mathbf{R})}{\partial R} \right|^2$$

and do not depend on the coordinate system.

Since the wave functions $\Psi_n^{x,y}(\mathbf{R},\mathbf{r})$ belong to the states with nonzero projections of the orbital angular momentum onto the $\mathbf{R}$-axis, these functions are zero if the vector $\mathbf{r}$ is directed along the vector $\mathbf{R}$. In the new coordinate system, the polar angles of these vectors are equal to $\pi/2$ in that event. Let us consider first the function Ψ_n^x. The associated Legendre polynomials, which are constituents of the Coulomb functions $\psi_{nlm}(\mathbf{r})$, and their derivatives at $\theta = \pi/2$ are equal to [84]

$$N_{lm} P_l^{|m|}(\cos\theta)\big|_{\cos\theta=0} = N_{lm}\, \frac{2^{|m|}}{\sqrt{\pi}}\, \frac{\Gamma\big[(l+|m|+1)/2\big]}{\Gamma\big[1+(l-|m|)/2\big]} \times \sin\left[\frac{\pi}{2}(l+|m|+1)\right], \qquad (51)$$

$$N_{lm} \frac{\mathrm{d}P_l^{|m|}(\cos\theta)}{\mathrm{d}\cos\theta}\bigg|_{\cos\theta=0} = N_{lm}\, \frac{2^{|m|+1}}{\sqrt{\pi}}\, \frac{\Gamma\big[1+\big(l+|m|\big)/2\big]}{\Gamma\big[\big(l-|m|+1\big)/2\big]} \times \sin\left[\frac{\pi}{2}\big(l+|m|\big)\right]. \qquad (52)$$

We see from the definition of $\Psi_n^x(\mathbf{R},\mathbf{r})$ that for $\mathbf{r}\|\mathbf{R}$ this function is proportional to the product of expressions (51), (52). The latter product, in turn, is proportional to the product of sines

$$\sin\left[\frac{\pi}{2}\big(l+|m|+1\big)\right] \sin\left[\frac{\pi}{2}\big(l+|m|\big)\right], \qquad (53)$$

which is zero for any integer l and m. In other words, in the sum defining the function Ψ_n^x either the function ψ_{nlm} or its derivative $\partial\psi_{nlm}/\partial\theta$ are zero at $\theta_r = \theta_R = \pi/2$.

The function $\Psi_n^y(\mathbf{R},\mathbf{r})$, which is given by the sum in formula (49), is also equal to zero for $\mathbf{r}\|\mathbf{R}$, when the azimuthal angles of these vectors are the same: $\phi_r = \phi_R$. The sum in Eqn (49) can be written as

$$\sum_{lm} \psi_{nlm}^*(\mathbf{r})\, \frac{\partial \psi_{nlm}(\mathbf{R})}{\partial \phi_R} = \frac{\mathrm{i}}{2\pi} \sum_{l=0}^{n-1} f_{nl}(r) f_{nl}(R) \sum_{m=-l}^{m=+l} m \big| N_{lm} P_l^{|m|}(0) \big|^2 = 0\,. \qquad (54)$$

The expression under the modulus sign in the last sum depends only on the absolute value $|m|$. After multiplication by m, the contributions to this sum from $+|m|$ and $-|m|$ cancel out for any $|m|$, and hence the entire sum becomes zero.

Functions (49) are mutually orthogonal. The corresponding integrals turn out to be proportional to expressions (53) and (54), which are zero. The functions $\Psi_n^{x,y}(\mathbf{R},\mathbf{r})$ for $L = 1$

are also orthogonal to $\Psi_n(\mathbf{R},\mathbf{r})$ for $L=0$, because they belong to the states with different projections of the angular momentum onto the internuclear axis. The integrals of $\Psi_n\Psi_n^x$ and $\Psi_n\Psi_n^y$ are proportional to the product of sines (53) and to the sum (54), respectively.

2.3 Properties of Coulomb Green functions and the complete basis of adiabatic wave functions

A Coulomb system possesses a symmetry which manifests itself in the degeneracy of its energy levels [7, 21]. This symmetry affects the properties of the Coulomb Green function whose spectral expansion (5) can be written as

$$\widetilde{G}(\mathbf{R},\mathbf{r},E)=\sum_n \frac{\sqrt{Q_n(R)}\,\Psi_n(\mathbf{R},\mathbf{r})}{E_n-E}\,, \tag{55}$$

where the functions $\Psi_n(\mathbf{R},\mathbf{r})$ are given by formula (27).

For each principal quantum number n, the linear combinations can be constructed from n^2 wave functions of degenerate states, which will become the wave functions in the new representation. One of these functions is $\Psi_n(\mathbf{R},\mathbf{r})$ which is present in the spectral expansion of the ionic function (26). The remaining functions, designated as $\Psi_{nlm}\bigl(\mathbf{R}(t),\mathbf{r}\bigr)$, take the form

$$\Psi_{nlm}\bigl(\mathbf{R}(t),\mathbf{r}\bigr)=\sum_{l',m'} C^{nlm}_{nl'm'}(\mathbf{R})\,\psi_{nl'm'}(\mathbf{r}) \tag{56}$$

and are not present in (55). The functions $\Psi_{nlm}(\mathbf{R},\mathbf{r})$ must be orthogonal between themselves and orthogonal to the function Ψ_n. Consequently, the degenerate Coulomb basis set can be reconstructed in such a way that only one of the new functions, viz. $\Psi_n(\mathbf{R},\mathbf{r})$, will be present in the spectral expansion of the Green function (5), while $\Psi_{nlm}(\mathbf{R},\mathbf{r})$ will be absent in the expansion of interest.

Turning back to our problem, we see that since there are no functions $\Psi_{nlm}(\mathbf{R},\mathbf{r})$ in the spectral expansion of the Green function, the ionic term interacts only with one covalent state, while the energies of the remaining degenerate states Ψ_{nlm} do not change and are equal to the unperturbed Coulomb energies $E_n^0=-Z^2/2n^2$. Nevertheless, the latter states are not absolutely passive. They can be occupied during capture processes (1) and (2), because their wave functions $\Psi_{nlm}\bigl(\mathbf{R}(t),\mathbf{r}\bigr)$ are time dependent and because the matrix element of the time derivative between them and the function $\Psi_n(\mathbf{R},\mathbf{r})$ is nonzero. Thus, the complete basis set of adiabatic states includes both Ψ_n and Ψ_{nlm} states, and our goal now is to construct the functions Ψ_{nlm}.

The possibility of reconstructing the Coulomb basis set of eigenfunctions to study electron scattering by a system composed of many small-sized potential wells was explored in works [17], but the specific algorithm for constructing an orthonormal basis set was not discussed in previous papers [3–6, 17].

To find the reconstructed orthonormal Coulomb basis set of eigenfunctions, we assume that one of the Coulomb functions, say the function $\psi_{n\lambda\mu}$, is orthogonal to $\Psi_n(\mathbf{R},\mathbf{r})$ from the outset, so that $J_{n\lambda\mu}(\mathbf{R})=0$. Let us consider the function combinations ($\{l,m\}\neq\{\lambda,\mu\}$):

$$L=0\colon\ \Psi_{nlm}(\mathbf{R},\mathbf{r})=\psi_{nlm}(\mathbf{r})-J_{nlm}(\mathbf{R})\bigl[\Psi_n(\mathbf{R},\mathbf{r})+\psi_{n\lambda\mu}(\mathbf{r})\bigr]\,, \tag{57}$$

$$L=1\colon\ \Psi^{x,y,z}_{nlm}(\mathbf{R},\mathbf{r})=\psi_{nlm}(\mathbf{r})-J^{x,y,z}_{nlm}(\mathbf{R})\bigl[\Psi^{x,y,z}_{n}(\mathbf{R},\mathbf{r})+\psi_{n\lambda\mu}(\mathbf{r})\bigr]. \tag{58}$$

Each of these functions is orthogonal to Ψ_n ($L=0$) or to $\Psi_n^{x,y,z}$ ($L=1$). For the mutual orthogonality, for example, of functions $\Psi_{nlm}(\mathbf{R},\mathbf{r})$ to be established, we must calculate the integral of their product:

$$\int\Psi_{nlm}\,\Psi^*_{nl'm'}\,\mathrm{d}\mathbf{r}=\delta_{ll'}\delta_{mm'}-2J_{nlm}\,J^*_{nl'm'}+J_{nlm}\,J^*_{nl'm'}\int\bigl|\Psi_n(\mathbf{R},\mathbf{r})+\psi_{n\lambda\mu}(\mathbf{r})\bigr|^2\,\mathrm{d}\mathbf{r}\,. \tag{59}$$

Since $\psi_{n\lambda\mu}(\mathbf{r})$ is orthogonal to $\Psi_n(\mathbf{R},\mathbf{r})$, the integral in the right-hand side of relation (59) is equal to 2 (functions $\psi_{n\lambda\mu}$ and Ψ_n are normalized to unity), and the sum of the second and third terms in formula (59) is zero. The same is true for the case of $L=1$; therefore, each of the functions (57) and (58) is normalized to unity and orthogonal to all the other functions:

$$\int\Psi^*_{nlm}(\mathbf{R},\mathbf{r})\Psi_{nl'm'}(\mathbf{R},\mathbf{r})\,\mathrm{d}\mathbf{r}=\delta_{ll'}\delta_{mm'}\,, \tag{60}$$

$$\int\bigl(\Psi^{x,y,z}_{nlm}(\mathbf{R},\mathbf{r})\bigr)^*\,\Psi^{x,y,z}_{nl'm'}(\mathbf{R},\mathbf{r})\,\mathrm{d}\mathbf{r}=\delta_{ll'}\delta_{mm'}\,. \tag{61}$$

At $l=\lambda$ and $m=\mu$, the equality $\Psi_{n\lambda\mu}=\psi_{n\lambda\mu}$ holds for the functions entering into Eqn (57), because $\psi_{n\lambda\mu}$ is orthogonal to Ψ_n ($L=0$) and the second term in formula (57) is zero. Therefore, the function (57) with orbital quantum numbers λ and μ is not orthogonal to the functions (57) with $l\neq\lambda$ and $\mu\neq m$. This is also true for the case of $L=1$. Consequently, for a given principal quantum number n, the number of orthonormal functions Ψ_{nlm} or $\Psi^{x,y,z}_{nlm}$ is n^2-1. Together with Ψ_n or $\Psi_n^{x,y,z}$, the total number of functions is n^2, as must be the case.

The proposed orthogonalization method [see formulas (57) and (58)] is general in character. It is based on the existence of the function $\psi_{n\lambda\mu}$ which is orthogonal to the active-state function Ψ_n from the outset. For this method to be applicable to our problem, it must be shown that the function $\psi_{n\lambda\mu}$ actually exists.

In the above-introduced coordinate system with the z-axis perpendicular to the collision plane, the polar angle θ_R of vector $\mathbf{R}$ is constant during the collision time and is equal to $\pi/2$. The functions $\psi_{nlm}(\mathbf{R})$ and their derivatives with respect to x and y are proportional to the associated Legendre polynomials when $\cos\theta=0$, while the derivatives with respect to z are proportional to the derivatives of these polynomials. These polynomials and their derivatives at $\theta=\pi/2$ are given by formulas (51) and (52), respectively. Thus, we see that $P_l^{|m|}(0)$ as well as $\psi_{nlm}(\mathbf{R})$ and its derivatives with respect to x and y become zero at even $l+|m|+1$, while the derivative with respect to z is zero at even $l+|m|$ (or odd $l+|m|+1$). The integrals $J_{nlm}(\mathbf{R})$ entering into formulas (28) and (49) vanish at these orbital quantum numbers l and m. Consequently, the Coulomb functions $\psi_{nlm}(\mathbf{r})$ with even $l+|m|+1$ are orthogonal to Ψ_n and $\Psi_n^{x,y}$ but not orthogonal to Ψ_n^z. At odd $l+|m|+1$, the functions $\psi_{nlm}(\mathbf{r})$ are orthogonal to Ψ_n^z and not orthogonal to Ψ_n and $\Psi_n^{x,y}$.

Thus, the function $\psi_{n\lambda\mu}(\mathbf{r})$ exists in our problem and is not unique. For each n, the number of such functions is approximately half the number of all degenerate states, i.e. $\approx n^2/2$. The states with these wave functions are strictly passive (see below).

As we see, the solution of the orthogonalization problem depends on the choice of the coordinate system. In the coordinate system we chose, this solution proves to be

simplest, because the polar angle θ_R of the vector $\mathbf{R}$ equals $\pi/2$ during the entire collision for both rectilinear and curvilinear trajectories. The trajectory must be merely planar, which is the case for central forces. The proposed method of constructing a complete orthonormal basis set is also based on the specific form of active-state functions $\Psi_n(\mathbf{R},\mathbf{r})$.

Each principal quantum number n has its own set of orthonormal functions $\{\Psi_n, \Psi_{nlm}\}$. Any function from the set relevant to n is orthogonal to any function from the set pertaining to n' ($n' \neq n$), because these sets are constructed from different sets of Coulomb functions (from ψ_{nlm} and $\psi_{n'lm}$, respectively) which are orthogonal between themselves.

The functions Ψ_{nlm} given by formula (57) for $L = 0$ become zero at $\mathbf{r} = \mathbf{R}$: $\Psi_{nlm}(\mathbf{r} = \mathbf{R}) = 0$. This fact is determined by the specific form of the active-state function Ψ_n and by its orthogonality to Ψ_{nlm}. In other words, it results from the degeneracy of Coulomb energy levels, which is attributable to Coulomb field symmetry [7, 21].

The ionic wave functions (26) and (45) are constructed from the wave functions of active states alone. Consequently, the wave function $\Psi_{nlm}(\mathbf{R},\mathbf{r})$ of any passive state is orthogonal to the ionic functions. By contrast, any active-state function is not orthogonal to the ionic functions (26) and (45). The integral of their product is equal to the coefficient $C_n(E)$ [see formulas (29) and (47)].

By using a procedure identical to that employed in constructing the orthonormal system of functions $\{\Psi_n, \Psi_{nlm}\}$ defined by formulas (57) and (58), here we examine the construction of the functions

$$L=0\colon\ \widetilde{\Psi}_n(\mathbf{R},\mathbf{r}) = \Psi_n(\mathbf{R},\mathbf{r}) - C_n(E)\left[\Phi(\mathbf{R},\mathbf{r}) + \psi_{n\lambda'\mu'}(\mathbf{r})\right], \tag{62}$$

$$L=1\colon\ \widetilde{\Psi}_n^{x,y,z}(\mathbf{R},\mathbf{r}) = \Psi_n^{x,y,z}(\mathbf{R},\mathbf{r}) - C_n^{x,y,z}(E)\left[\Phi_{x,y,z}(\mathbf{R},\mathbf{r}) + \psi_{n\lambda'\mu'}(\mathbf{r})\right], \tag{63}$$

where $\psi_{n\lambda'\mu'}$ is orthogonal to Ψ_n and Φ ($L = 0$) or to $\Psi_n^{x,y,z}$ and $\Phi_{x,y,z}$ ($L = 1$) (the orbital quantum numbers λ', μ' differ from λ, μ). The functions $\widetilde{\Psi}_n$ and $\widetilde{\Psi}_n^{x,y,z}$ are orthogonal between themselves and to the ionic functions Φ and $\Phi_{x,y,z}$ and orthogonal to the functions of passive states Ψ_{nlm} or $\Psi_{nlm}^{x,y,z}$ ($\lambda \neq \lambda', \mu \neq \mu'$). In addition, the functions (62) and (63) are normalized, because one has

$$\int \left|\widetilde{\Psi}_n(\mathbf{R},\mathbf{r})\right|^2 \mathrm{d}\mathbf{r} = \int \left|\Psi_n(\mathbf{R},\mathbf{r})\right|^2 \mathrm{d}\mathbf{r} = 1\,, \tag{64}$$

and a similar relation holds for $L = 1$.

The adiabatic matrix elements of the time derivative between the wave functions of active and passive states are defined as follows

$$L=0\colon\ V_{n,nlm}(\mathbf{R}) \equiv \int \Psi_{nlm}(\mathbf{R},\mathbf{r})\,\frac{\mathrm{d}\Psi_n(\mathbf{R},\mathbf{r})}{\mathrm{d}t}\,\mathrm{d}\mathbf{r} = \frac{\mathrm{d}J_{nlm}(\mathbf{R})}{\mathrm{d}t}, \tag{65}$$

$$L=1\colon\ V_{n,nlm}^{x,y,z}(\mathbf{R}) = \int \Psi_{nlm}^{x,y,z}(\mathbf{R},\mathbf{r})\,\frac{\mathrm{d}\Psi_n^{x,y,z}(\mathbf{R},\mathbf{r})}{\mathrm{d}t}\,\mathrm{d}\mathbf{r} = \frac{\mathrm{d}J_{nlm}^{x,y,z}(\mathbf{R})}{\mathrm{d}t}\,. \tag{66}$$

Matrix elements (65) and (66) do not depend on quantum numbers λ, μ. For $l = \lambda$ and $m = \mu$, matrix elements (65) and (66) become zero, because for these states the integrals $J_{nlm}(R)$ and $J_{nlm}^{x,y,z}(R)$ are equal to zero at any instant of time. Consequently, the states with quantum numbers $n\lambda\mu$ are strictly passive: their energies do not change in time and they are not occupied in collisions (1).

2.4 Sums of Coulomb wave function products over degenerate states and the properties of active-state wave functions

Let us calculate the sums of products of the Coulomb wave functions with negative energies, the sums taken over orbital quantum numbers l, m. These sums are present in formulas for adiabatic wave functions of covalent states, constructed in previous sections. Here we consider first the sum

$$\widehat{Q}_n(\mathbf{r},\mathbf{R}) = \sum_{lm} \psi_{nlm}^*(\mathbf{r})\,\psi_{nlm}(\mathbf{R}) \tag{67}$$

which is proportional to the wave function (27) of an active state. This sum can be expressed through a quadratic form of wave function of only one state with zero quantum numbers $l = m = 0$, i.e. through the function $\psi_{n0}(r)$ [11–13]. In V A Fock's papers [21] devoted to the four-dimensional symmetry of the atomic hydrogen, an analogous sum was investigated but for the wave functions in the momentum representation.

The sum (67) and a number of other sums can be calculated by comparing the limit of the Hostler–Pratt Coulomb Green function (6) as $E \to E_n$ with the analogous limit of the spectral expansion (5) of this function. The limit of the Coulomb Green function (6) as $E \to E_n$ has been discussed in paper [22] and has been used in calculations of the Born cross sections for transitions between the excited states of atomic hydrogen, which are caused by electron impacts [23–25]. In the linear combination (14), the first term is the leading one as $E \to E_n$, and the second term can be neglected. In formula (15) the term G_2 can also be neglected.

In the calculation of the Green function limit we shall use the following expression for the gamma-function in the resonant limit when $Zv \to n$ [84]:

$$\Gamma(1 - Zv_-) \to \frac{(-1)^n Z^2}{n^3(n-1)!}\,\frac{1}{E - E_n}\,. \tag{68}$$

Using this expansion we obtain for the resonant term:

$$G(\mathbf{r},\mathbf{R},E \to E_n) \approx \frac{1}{E-E_n}\sum_{l,m}\psi_{nlm}^*(\mathbf{r})\,\psi_{nlm}(\mathbf{R}) = \frac{1}{E-E_n}\,\frac{Z^2}{\pi n^3 n!(n-1)!}\,\frac{n}{x-y}\left(\frac{\partial}{\partial(Zy)} - \frac{\partial}{\partial(Zx)}\right) \times W_{n,1/2}\left(\frac{Zx}{n}\right) W_{n,1/2}\left(\frac{Zy}{n}\right), \tag{69}$$

whence it follows that

$$\hat{Q}_n(\mathbf{r},\,\mathbf{R}) = \sum_{l,m}\psi_{nlm}^*(\mathbf{r})\,\psi_{nlm}(\mathbf{R}) = \frac{Z^2}{\pi n^3 n!(n-1)!}\,\frac{n}{x-y}\left(\frac{\partial}{\partial(Zy)} - \frac{\partial}{\partial(Zx)}\right) \times W_+\left(\frac{Zx}{n}\right) W_+\left(\frac{Zy}{n}\right). \tag{70}$$

In the limit $E \to E_n$ ($Zv \to n$), the Whittaker function $W_{n,1/2}$ becomes proportional to the Coulomb wave function ϕ_{n0} with zero orbital quantum numbers $l = m = 0$:

$$W_{n,1/2}(r) = (-1)^{n+1} n! \sqrt{\frac{4\pi n}{Z}}\, \phi_{n0}(r)\,, \quad \phi_{n0}(r) \equiv r\,\frac{f_{n0}(r)}{\sqrt{4\pi}}\,. \tag{71}$$

This relation follows, for example, from the comparison of the asymptotic expressions of the functions $W_{Zv,1/2}(r)$ and $\phi_{n0}(r)$ as $r \to \infty$. Substituting formula (71) into (70) we obtain for the sum (67) [11, 12]:

$$\hat{Q}_n(\mathbf{r},\mathbf{R}) \equiv \sum_{l,m} \psi^*_{nlm}(\mathbf{r})\,\psi_{nlm}(\mathbf{R}) = \frac{4Z^2}{n^2}\,\frac{\phi'_{n0}(\tau_y)\,\phi_{n0}(\tau_x) - \phi_{n0}(\tau_y)\,\phi'_{n0}(\tau_x)}{\tau_x - \tau_y}\,, \tag{72}$$

where

$$\tau_x = \frac{ZR}{n}(1+\xi)\,, \quad \tau_y = \frac{ZR}{n}(1+\eta)\,,$$

and ξ, η are the elliptic coordinates introduced in Section 2.1.

By analyzing a Taylor expansion of the sum (72), we can obtain the sums of products of the arbitrary-order derivatives of Coulomb eigenfunctions with respect to the internuclear distance R at $\mathbf{r} = \mathbf{R}$ [8, 13]:

$$Q_n^{i,j}(R) = \sum_{l,m} \frac{\mathrm{d}^i \psi^*_{nlm}(\mathbf{R})}{\mathrm{d}R^i}\,\frac{\mathrm{d}^j \psi_{nlm}(\mathbf{R})}{\mathrm{d}R^j}\,. \tag{73}$$

To calculate the sum (73), let us consider the passage to the limit of relation (72) for $\mathbf{r} \to \mathbf{R}$, when the point $\mathbf{r}$ moves along the vector $\mathbf{R}$ and when $\tau_x = 2ZR/n = \text{const}$, $\tau_y = 2Zr/n$, and $\tau_x - \tau_y = 2Z(R-r)/n$. The expansion of the sum entering into Eqn (72) in a Taylor series in powers of $(r-R)$ takes the form

$$\sum_{l,m} \psi^*_{nlm}(\mathbf{r})\,\psi_{nlm}(\mathbf{R}) \approx \sum_{l,m} \left|\psi_{nlm}(\mathbf{R})\right|^2 + (r-R)\sum_{l,m} \frac{\mathrm{d}\psi_{nlm}(\mathbf{R})}{\mathrm{d}R}\,\psi^*_{nlm}(\mathbf{R}) + \ldots + \frac{(r-R)^k}{k!}\sum_{l,m} \frac{\mathrm{d}^k\psi_{nlm}(\mathbf{R})}{\mathrm{d}R^k}\,\psi^*_{nlm}(\mathbf{R}) + \ldots \tag{74}$$

and the analogous expansion of the right-hand part in formula (72) is

$$\frac{\phi'_{n0}(r)\,\phi_{n0}(R) - \phi_{n0}(r)\,\phi'_{n0}(R)}{R-r} = \left(\frac{\mathrm{d}\phi_{n0}(R)}{\mathrm{d}R}\right)^2 - \phi_{n0}(R)\,\frac{\mathrm{d}^2\phi_{n0}(R)}{\mathrm{d}R^2} + \ldots + \frac{(r-R)^{k-1}}{k!} \times \left(\phi'_{n0}(R)\,\frac{\mathrm{d}^k\phi_{n0}(R)}{\mathrm{d}R^k} - \phi_{n0}(R)\,\frac{\mathrm{d}^{k+1}\phi_{n0}(R)}{\mathrm{d}R^{k+1}}\right) + \ldots \tag{75}$$

Comparing these two expansions and equating the terms at the same powers of $(r-R)$ one arrives at

$$Q_n^{(0,j)}(R) \equiv \sum_{lm} \psi^*_{nlm}(\mathbf{R})\,\frac{\mathrm{d}^j\psi_{nlm}(\mathbf{R})}{\mathrm{d}R^j} = \frac{1}{j+1}\left(\phi_{n0}^{(j+1)}(R)\,\phi_{n0}^{(1)}(R) - \phi_{n0}^{(j+2)}(R)\,\phi_{n0}(R)\right), \tag{76}$$

where $\phi^{(j)} \equiv \mathrm{d}^j\phi/\,\mathrm{d}^j R$.

For the special cases of $j = 0$ and $j = 1$ we obtain from relation (76) two sums:

$$Q_n^{(0,0)}(R) \equiv \sum_{l,m} \left|\psi_{nlm}(\mathbf{R})\right|^2 = \sum_{l=0}^{n-1} \frac{2l+1}{4\pi} f_{nl}^2(R) = \left(\phi'_{n0}(R)\right)^2 + 2\left(E_n + \frac{Z}{R}\right)\phi_{n0}^2(R)\,, \tag{77}$$

$$Q_n^{(0,1)}(R) \equiv \sum_{lm} \psi^*_{nlm}(\mathbf{R})\,\frac{\mathrm{d}\psi_{nlm}(\mathbf{R})}{\mathrm{d}R} = \sum_{l=0}^{n-1} \frac{2l+1}{4\pi} f_{nl}(R)\,\frac{\mathrm{d}f_{nl}(R)}{\mathrm{d}R} = -Z\psi_{n0}^2(R)\,. \tag{78}$$

The sum $Q_n(R)\left(\equiv Q_n^{(0,0)}(R)\right)$ is shown in Fig. 3.

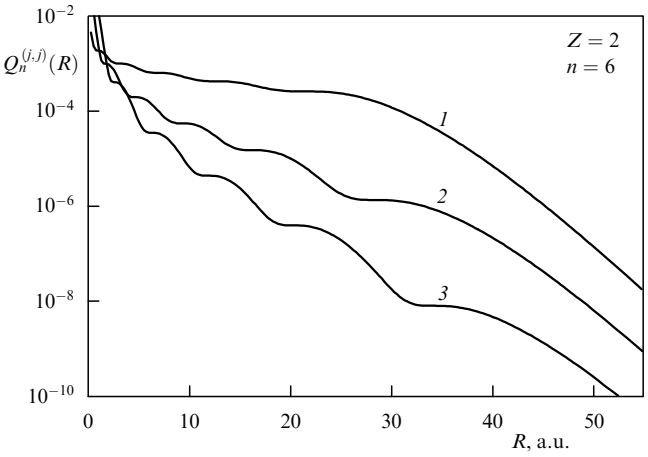

Figure 3. Sums $Q_n^{(j,j)}(R)$ as the functions of distance R from the nucleus of $He^{+,*}(n)$: *1* — $Q_n(R)$, *2* — $Q_n^{(1,1)}$, *3* — $Q_n^{(2,2)}$ [equations (77), (89) and (90), respectively].

The above-calculated sums make it possible to investigate the properties of the wave function of an active state:

$$\Psi_n(\mathbf{R},\mathbf{r}) = \frac{2Z}{n}\,\frac{\phi'_{n0}(\tau_y)\,\phi_{n0}(\tau_x) - \phi_{n0}(\tau_y)\,\phi'_{n0}(\tau_x)}{|\mathbf{R}-\mathbf{r}|\sqrt{Q_n(R)}}\,. \tag{79}$$

At the point $\mathbf{r} = \mathbf{R}$, the denominator in formula (79) comes to nought but the function Ψ_n does not go to infinity, because the numerator in Eqn (79) is also equal to zero at this point. Indeed, at the point $\mathbf{r} = \mathbf{R}$, the variables τ_x and τ_y are equal: $\tau_x = \tau_y = 2ZR/n$, and the numerator in formula (79) becomes the Wronskian of the same function ϕ_{n0}.

For investigating in detail the properties of the wave function (79) we use the following expression for the normalized function ϕ_{n0}:

$$\phi_{n0}(\tau) = \sqrt{\frac{Z}{4\pi n}}\,\tau \exp\left(-\frac{\tau}{2}\right) F(-n+1, 2, \tau)\,. \tag{80}$$

The function (79) depends on two-center elliptic coordinates ξ, η. The first center is placed at the nucleus of the positive ion, and the second center — at the nucleus of the negative ion. This function is not symmetrical relative to the plane which is perpendicular to the internuclear axis $\mathbf{R}$ and goes through the positive ion nucleus (see Fig. 4).

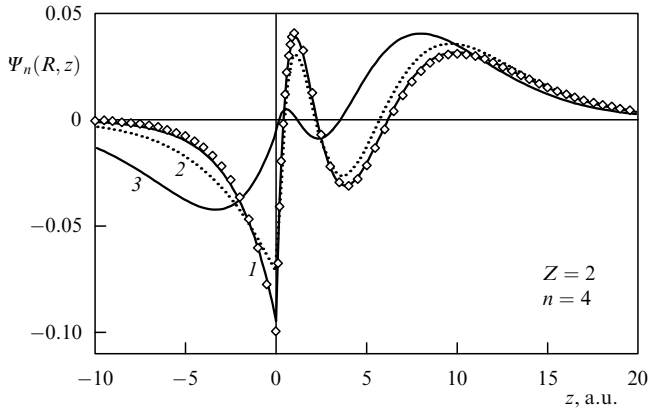

Figure 4. Wave function of the active state $\Psi_n(R,z)$ [$L=0$, formula (79)] for $Z=2$ and $n=4$ (orbit size $r_n=2n^2/Z=16$) versus the distance z from the nucleus He^{++} along the internuclear axis $\mathbf{R}$ for three values of internuclear distance R: *1* — $R=+4r_n=+64$ (thick solid line); *2* — $R=r_n=+16$ (dotted line); *3* — $R=r_n/2=+8$ (thin solid line); diamonds mark asymptotic limit (85).

At internuclear distances which are much larger than the size of the nth Coulomb orbit $r_n=2n^2/Z$, viz. $R\gg r_n$, the elliptic coordinates ξ,η are close to the parabolic coordinates $\tilde{\mu}=r+z$, $\tilde{\nu}=r-z$ in the vicinity of the positive ion:

$$\xi\approx 1-\frac{\tilde{\nu}}{R}+\dots\,,\qquad \eta\approx -1+\frac{\tilde{\mu}}{R}+\dots$$

At these distances, the function (79) of the active state is transformed in the vicinity of the positive ion to the Coulomb eigenfunction in parabolic coordinates.

Indeed, at large R the variable τ_x is also large and, consequently, for the function $\phi_{n0}(\tau_x)$ we can take advantage of the asymptotic expansion into a series in inverse powers of R:

$$\begin{aligned} &R\to\infty: \qquad \tau_x\approx\frac{2ZR}{n}+\frac{Z\tilde{\nu}}{n}+\dots\,,\\ &\phi_{n0}(\tau_x)\approx\exp\left(-\frac{Z\tilde{\nu}}{2n}\right)\phi_{n0}^{\mathrm{as}}\left(\frac{2ZR}{n}\right), \end{aligned} \tag{81}$$

where we set

$$\phi_{n0}^{\mathrm{as}}\left(\frac{2ZR}{n}\right)=\frac{1}{n!}\sqrt{\frac{Z}{4\pi n}}\left(\frac{2ZR}{n}\right)^n\exp\left(-\frac{ZR}{n}\right),$$

and the asymptotic expansion of the derivative yields $\phi'_{n0}(\tau_x)\approx-\phi_{n0}(\tau_x)/2$. Asymptotic expansion of the function $\phi_{n0}(\tau_y)$ is not possible, because the variable τ_y is not large as $R\to\infty$, and we then have

$$\begin{aligned} \Psi_n(\mathbf{R},\mathbf{r})\approx\frac{Z}{nR}\,\frac{1}{\sqrt{Q_n(R)}}\,\phi_{n0}\left(\frac{2ZR}{n}\right)\\ \times\exp\left(-\frac{Z\tilde{\nu}}{2n}\right)\left[2\phi'_{n0}\left(\frac{Z\tilde{\mu}}{n}\right)+\phi_{n0}\left(\frac{Z\tilde{\mu}}{n}\right)\right]. \end{aligned} \tag{82}$$

Hence it follows that at large R the active-state function $\Psi_n(\mathbf{R},\mathbf{r})$ was transformed to a product of functions depending on parabolic coordinates $\tilde{\nu}$ and $\tilde{\mu}$. Coulomb wave functions in parabolic coordinates are linear combinations of spherical functions with Clebsch – Gordan coefficients [30]. By inverse transformation of these combinations, the wave function $\Psi_n(\mathbf{R},\mathbf{r})$ can be expanded in terms of eigenfunctions expressed in parabolic coordinates at any value of R.

In order to proceed to the limit of this expansion as $R\to\infty$, we should investigate expression (82) in more details. Making use of the asymptotic limit of the sum:

$$\begin{aligned} Q_n(R)\to n\psi_{n0}^2(R)\approx\frac{1}{(n!)^2}\,\frac{Z^3}{\pi n^2}\left(\frac{2ZR}{n}\right)^{2n-2}\\ \times\exp\left(-\frac{2ZR}{n}\right),\quad R\to\infty, \end{aligned} \tag{83}$$

we transform expression (82) to the form

$$\begin{aligned} \Psi_n(\mathbf{R},\mathbf{r})\approx\frac{Z}{n\sqrt{n}}\exp\left(-\frac{Z\tilde{\nu}}{2n}\right)\\ \times\left[2\phi'_{n0}\left(\frac{Z\tilde{\mu}}{n}\right)+\phi_{n0}\left(\frac{Z\tilde{\mu}}{n}\right)\right],\quad R\to\infty. \end{aligned} \tag{84}$$

For subsequent transformations we calculate the derivative of function (80) and take advantage of the functional relations 9.212.2, 9.212.3, 9.213 between confluent hypergeometrical functions compiled in the handbook [84]. As a result we found that the function $\Psi_n(\mathbf{R},\mathbf{r})$ transforms in the limit $R\to\infty$ to the wave function of a Stark state with quantum numbers $n, m=0, n_1=n-1, n_2=0$:

$$\begin{aligned} \Psi_n(\mathbf{R},\mathbf{r})\approx\psi_{n,m,n_1}(\tilde{\mu},\tilde{\nu})=\frac{Z^{3/2}}{n^2\sqrt{\pi}}\exp\left(-\frac{Zr}{n}\right)\\ \times F_1\left(-n+1,1,\frac{Z\tilde{\mu}}{n}\right). \end{aligned} \tag{85}$$

This state possesses the maximum dipole moment $d_n^{\max}=3n(n-1)/2Z$ [7] and the center of the electron charge in this state is displaced to the negative ion.

Function (79) and its limiting expression (85) are shown in Fig. 4 as a function of distance z (reckoned from the nucleus of the positive ion) along the internuclear axis. Function (79) is plotted for three values of distance R. It follows from this figure that for large internuclear distances $R\gg r_n$ function (79) is asymmetric relative to the point $z=0$ and is close to its limit defined by Eqn (85).

Stark states constitute Rydberg states of atomic hydrogen and hydrogen-like ions perturbed by a weak uniform electric field $\mathbf{F}$ [7]. In these states, electrons have dipole moments $d_n=-3n(n_1-n_2)/2Z$ and their energy level shifts are the linear functions of F: $E-E_n=\ =3Fn(n_1-n_2)/2Z$. If hydrogen Rydberg atoms are perturbed by a positive atomic ion with charge $\tilde{Z}$, then at large internuclear distances the electric field of the ion is $F\sim\tilde{Z}R^{-2}$ and the shifts of Rydberg energy levels are $E-E_n\approx 3n\tilde{Z}(n_1-n_2)/2ZR^2$ [15].

In the case under consideration the Rydberg atoms are formed in the final states accompanying collision (1), when there is no electric field. For example, in the collision $H^-+He^{++}=H(1s)+He^{+,*}(nlm)$, final Rydberg states of the helium ion interact with atomic hydrogen in the ground state. Nevertheless, in our approach the wave function of the active state $\Psi_n(\mathbf{R},\mathbf{r})$ is transformed as $R\to\infty$ to the wave function of the Stark state which has the maximum dipole moment for a given principal quantum number n. This fact is the consequence of the degeneracy peculiar to Coulomb energy levels that manifests itself in specific features of the Coulomb Green function.

We also emphasize that because of the specific feature of the active wave function, pointed out above, a couple of

atoms are formed in the recombination reaction (1), one of which possesses a dipole moment. The interaction energy of electrons in such atoms is increased at large distances R. For example, at the collision $H_a^- + H_b^+$, the system $H_a(1s) + H_b^*(n)$ is formed after the outer electron exchange. The interaction energy between the core $1s$-electron of the atom $H_a(1s)$ and the dipole moment of the Rydberg atom $H_b^*(n)$ is inversely proportional to the internuclear distance squared, viz. $\simeq R^{-2}$. However, the proton of the atom H_a also interacts with the dipole moment of the atom H_b and the term $\sim R^{-2}$ is absent in the total interatomic interaction energy (in the molecular term).

The dipole moment of the quantum system is defined as

$$d_n(R) = \int\int\int z\left|\Psi(\mathbf{R},\mathbf{r})\right|^2 \mathrm{d}^3 r\,. \tag{86}$$

Dipole moments $d_n(R)$ of active states $\Psi_n(\mathbf{R},\mathbf{r})$ [$L=0$, formula (79)] and $\Psi_n^{x,y,z}(\mathbf{R},\mathbf{r})$ [$L=1$, formulas (95) and (96)] have been calculated numerically on the basis of integral (86). The calculated results are shown in Fig. 5. Dipole moments are present in this figure as functions of an internuclear distance R for the Rydberg states with principal quantum number $n=4$ and for the charge $Z=2$ of a positive ion.

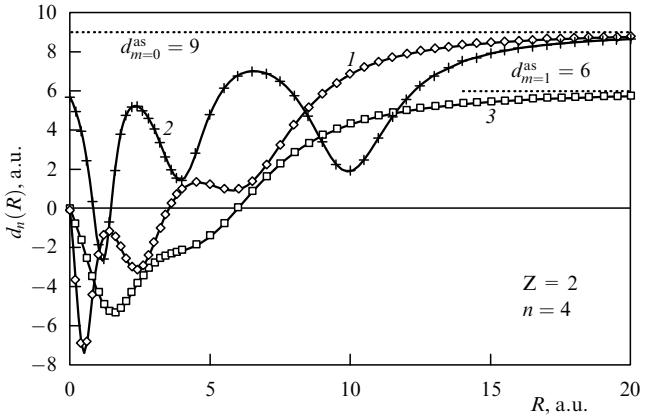

Figure 5. Dipole moments $d_n(R)$ of active covalent states for $Z=2$, $n=4$ as a function of internuclear distance R. The lines were calculated by means of sums (87), (104) and (108); crosses, squares and diamonds — by numerical integration with formula (86). Curve *1* — the state $\Psi_n(\mathbf{R},\mathbf{r})$ defined by formula (79); curve *2* — the state $\Psi_n^z(\mathbf{R},\mathbf{r})$ specified by formula (95), and curve 3 — the state $\Psi_n^{x,y}(\mathbf{R},\mathbf{r})$ defined by formula (96).

Integral (86) can be calculated analytically; the result of this computation is described by a sum over the orbital quantum number l. Making use of the radial matrix element $\langle n, l-1|r|n,l\rangle = -(3n/2Z)\sqrt{n^2-l^2}$ [31] and the integral of the associated Legendre polynomials product [32] we obtain the dipole moment for the state $\Psi_n(\mathbf{R},\mathbf{r})$:

$$d_n(R) = -\frac{3n}{4\pi Z Q_n(R)} \sum_{l=0}^{n-1} l\sqrt{n^2-l^2}\, f_{n,l}(R)\, f_{n,l-1}(R). \tag{87}$$

Dipole moments calculated using this sum are shown in Fig. 5 as a function of distance R. It is clearly seen that the results derived with integral (86) and with sum (87) are the same. In the limit of large distances $R\to\infty$, the dipole moment for the active state $\Psi_n(\mathbf{R},\mathbf{r})$ indeed has a maximum value for $n=4$ and $Z=2$: $d_n^{\mathrm{as}} = 3n(n-1)/2Z = 9$ a.u.

The sums $Q_n^{(0,j)}$ with arbitrary j can be expressed through quadratic forms involving only the function $\phi_{n0}(r)$ and its first derivative $\phi'_{n0}(r)$. These sums with $j=2-5$ have been taken in papers [8, 13].

The sums of products of wave function derivatives are obtained by differentiating equation (76) with respect to R:

$$\begin{aligned} Q_n^{(1,j)}(R) &\equiv \sum_{l,m} \frac{\mathrm{d}\psi_{nlm}^*}{\mathrm{d}R}\,\frac{\mathrm{d}^j\psi_{nlm}(\mathbf{R})}{\mathrm{d}R^j} \\ &= \frac{\phi_{n0}^{(2)}(R)\,\phi_{n0}^{(j+1)}(R)}{j+1} - \frac{\phi_{n0}^{(1)}(R)\,\phi_{n0}^{(j+2)}(R)}{j+2} \\ &\quad - \frac{\phi_{n0}(R)\phi_{n0}^{(j+3)}(R)}{(j+1)(j+2)}\,, \end{aligned} \tag{88}$$

$$\begin{aligned} Q_n^{(2,j)}(R) &\equiv \sum_{l,m} \frac{\mathrm{d}^2\psi_{nlm}^*}{\mathrm{d}R^2}\,\frac{\mathrm{d}^j\psi_{nlm}(\mathbf{R})}{\mathrm{d}R^j} \\ &= \frac{\phi_{n0}^{(3)}(R)\phi_{n0}^{(j+1)}(R)}{j+1} - \frac{j\phi_{n0}^{(2)}(R)\phi_{n0}^{(j+2)}(R)}{(j+1)(j+2)} \\ &\quad - \frac{2\phi_{n0}^{(1)}(R)\,\phi_{n0}^{(j+3)}(R)}{(j+1)(j+3)} - \frac{2\phi_{n0}(R)\,\phi_{n0}^{(j+4)}(R)}{(j+1)(j+2)(j+3)}\,. \end{aligned} \tag{89}$$

By continuing the differentiation, we can take the sums $Q_n^{(i,j)}$ with arbitrary values of i and j. However, the expressions quickly become unwieldy.

When investigating collisions (1) and (2) we need to know the following sums:

$$\begin{aligned} Q_n^{(1,1)}(R) &= \sum_{l,m}\left|\frac{\mathrm{d}\psi_{nlm}(\mathbf{R})}{\mathrm{d}R}\right|^2 = \sum_l \frac{2l+1}{4\pi}\left(\frac{\mathrm{d}f_{nl}(R)}{\mathrm{d}R}\right)^2 \\ &= \frac{2}{3}\left[\left(E_n + \frac{Z}{R}\right)Q_n^{(0,0)}(R) - \frac{Z}{R}\,\frac{\mathrm{d}}{\mathrm{d}R}\left(\frac{\phi_{n0}^2(R)}{R}\right)\right], \end{aligned} \tag{90}$$

$$\begin{aligned} Q_n^{(2,2)}(R) &= \sum_{l,m}\left|\frac{\mathrm{d}^2\psi_{nlm}(\mathbf{R})}{\mathrm{d}R^2}\right|^2 = \sum_l \frac{2l+1}{4\pi}\left(\frac{\mathrm{d}^2 f_{nl}(R)}{\mathrm{d}R^2}\right)^2 \\ &= \frac{4}{5}\left\{\left[\left(E_n + \frac{Z}{R}\right)^2 + \frac{2Z}{R^3}\right]Q_n^{(0,0)}(R)\right. \\ &\quad - \frac{Z}{R^3}\left[8\left(E_n + \frac{Z}{R}\right) - \frac{Z}{R} - \frac{2}{R^2}\right]\phi_{n0}^2(R) \\ &\quad \left. + \frac{2Z}{R^2}\left[E_n + \frac{Z}{R} - \frac{2}{R^2}\right]\phi_{n0}(R)\,\phi'_{n0}(R)\right\}, \end{aligned} \tag{91}$$

which are determined through the use of expressions (88) and (89) during calculation of higher-order derivatives of the function $\phi_{n0}(r)$.

Differentiating relation (90) with respect to R we obtain a simple expression for the sum with $i=1, j=2$:

$$\begin{aligned} Q_n^{(1,2)}(R) &\equiv \sum_{l,m}\frac{\mathrm{d}\psi_{nlm}^*(\mathbf{R})}{\mathrm{d}R}\,\frac{\mathrm{d}^2\psi_{nlm}(\mathbf{R})}{\mathrm{d}R^2} = \frac{1}{2}\,\frac{\mathrm{d}}{\mathrm{d}R}\,Q_n^{(1,1)}(R) \\ &= -Z\,\psi'^2_{n0}(R)\,. \end{aligned} \tag{92}$$

The differentiation of relation (91) gives the simple expression for the sum with $i=2, j=3$:

$$\begin{aligned} Q_n^{(2,3)}(R) &\equiv \sum_{l,m}\frac{\mathrm{d}^2\psi_{nlm}^*(\mathbf{R})}{\mathrm{d}R^2}\,\frac{\mathrm{d}^3\psi_{nlm}(\mathbf{R})}{\mathrm{d}R^3} = \frac{1}{2}\,\frac{\mathrm{d}}{\mathrm{d}R}\,Q_n^{(2,2)}(R) \\ &= -Z\,\psi''^2_{n0}(R) - \frac{4Z^2}{5R^4}\left(\phi_{n0}^2(R)\right)'. \end{aligned} \tag{93}$$

Using relations (78), (92) and (93) we can express the sums $Q_n(\equiv Q_n^{(0,0)})$, $Q_n^{(1,1)}$ and $Q_n^{(2,2)}$ through the following integrals:

$$Q_n(R) = 2Z\int_R^\infty \psi_{n0}^2(r)\,\mathrm{d}r\,,$$
$$Q_n^{(1,1)}(R) = 2Z\int_R^\infty \psi_{n0}'^2\,\mathrm{d}r\,,$$
$$Q_n^{(2,2)}(R) = 2Z\int_R^\infty \left\{\psi_{n0}''^2(r) + \frac{4Z}{5r^4}\left(\phi_{n0}^2(r)\right)'\right\}\mathrm{d}r\,. \qquad (94)$$

The sums $Q_n(R), Q_n^{(1,1)}(R)$ and $Q_n^{(2,2)}(R)$ are shown in Fig. 3 as a function of the internuclear distance R. These sums are present in the normalization factors of wave functions of active states for negative ions with orbital momenta $L = 0$, 1 and 2. They do not have zeros at finite values of R and decrease by steps when R is increased. It follows from relations (78), (92)–(94) that the derivatives of these sums are equal to zero at the central point of each step. The calculated sums are interesting for the physics of negative and positive ion collisions and for the physics of highly excited Rydberg atoms [26], specifically, for investigations into the broadening and shift of spectral lines corresponding to radiative transitions involving Rydberg states.

The expressions for wave functions of active states in a negative ion with an orbital momentum $L = 1$ participating in collisions (1) were obtained from the analysis of the limit of Coulomb Green function derivatives at $E \to E_n$ [8]. These wave functions are as follows

$$\Psi_n^z(\mathbf{R},\mathbf{r}) \equiv \sum_{l,m} \frac{\psi_{nlm}^*(\mathbf{r})}{\sqrt{Q_n^{(1,1)}(R)}}\,\frac{\mathrm{d}\psi_{nlm}(\mathbf{R})}{\mathrm{d}R}$$
$$= \frac{4Z^2\cos\theta_b}{n^2|\mathbf{r}-\mathbf{R}|\sqrt{Q_n^{(1,1)}(R)}}$$
$$\times\left[\frac{n^2\sqrt{Q_n(R)}}{4Z^2}\,\Psi_n(\mathbf{R},\mathbf{r}) - \phi_{n0}'(\tau_x)\,\phi_{n0}'(\tau_y)\right.$$
$$\left.+\left(\frac{1}{4} - \frac{n^2(R-r)}{2ZR(R-z)}\right)\phi_{n0}(\tau_x)\,\phi_{n0}(\tau_y)\right], \qquad (95)$$

$$\Psi_n^{x,y}(\mathbf{R},\mathbf{r}) \equiv \sum_{l,m} \frac{\psi_{nlm}^*(\mathbf{r})}{\sqrt{Q_n^{(\theta,\theta)}(R)}}\,\frac{\partial\psi_{nlm}(\mathbf{R})}{\partial\{x,y\}}$$
$$= \frac{4Z^2\sin\theta_b\{\cos\phi_b,\sin\phi_b\}}{n^2|\mathbf{r}-\mathbf{R}|\sqrt{Q_n^{(\theta,\theta)}(R)}}$$
$$\times\left[\frac{n^2\sqrt{Q_n(R)}}{4Z^2}\,\Psi_n(\mathbf{R},\mathbf{r}) - \phi_{n0}'(\tau_x)\,\phi_{n0}'(\tau_y)\right.$$
$$\left.+\left(\frac{1}{4} - \frac{n^2(r+R)}{2ZR(r+z)}\right)\phi_{n0}(\tau_x)\,\phi_{n0}(\tau_y)\right], \qquad (96)$$

where $\Psi_n(\mathbf{R},\mathbf{r})$ is given by formula (79). The functions (95) and (96) are regular at $\mathbf{r} = \mathbf{R}$. The sum $Q_n^{(1,1)}(R)$ was calculated above.

The sum $Q_n^{(\theta,\theta)}$ assumes the form

$$Q_n^{(\theta,\theta)}(R) = \frac{1}{R^2}\sum_{l,m}\left|\frac{\partial\psi_{nlm}(\mathbf{R})}{\partial\theta}\right|_{\theta=0}^2. \qquad (97)$$

This sum cannot be calculated by leaning upon the Coulomb Green function analysis. We should analyze the derivative of the associated Legendre polynomials at $\theta \approx 0$. Making use of the appropriate formulation of these polynomials [84] we obtain that for any orbital momentum l the derivative of the polynomial with respect to angle θ is not equal to zero at $\theta = 0$ only for the projections $m = \pm 1$ of an orbital momentum. This derivative is defined in the following way:

$$\left.\frac{\mathrm{d}P_l^1(\cos\theta)}{\mathrm{d}\theta}\right|_{\theta=0} = -\frac{1}{2}\,l(l+1)\,. \qquad (98)$$

With the last derivative we transform the sum (97) to the form

$$Q_n^{(\theta,\theta)}(R) = \frac{1}{8\pi R^2}\sum_l (2l+1)\,l(l+1)f_{nl}^2(R)\,. \qquad (99)$$

The subsequent calculation of the sum (99) is connected with the calculation of the following sum: $\sum_{l,m} l(l+1)\left|\psi_{nlm}(\mathbf{R})\right|^2$. By means of the addition theorem for spherical harmonics (31), the latter sum can be written in the form

$$Q_n^{(l,l+1)}(R) \equiv \sum_{l,m} l(l+1)\left|\psi_{nlm}(\mathbf{R})\right|^2$$
$$= \frac{1}{4\pi}\sum_l (2l+1)\,l(l+1)f_{nl}^2(R)\,. \qquad (100)$$

The sums (99) and (100) differ in the multiplier $1/2R^2$ which does not depend on the quantum numbers l, m. Consequently, after calculation of the sum (100) we shall also find the sum (99).

For taking the sum (100) we express the product $l(l+1)f_{nl}$ through the f_{nl}, $\mathrm{d}f_{nl}/\mathrm{d}R$ and $\mathrm{d}^2f_{nl}/\mathrm{d}R^2$ using the wave equation for the radial wave function f_{nl} [7]. Then the sums (99) and (100) are expressed through those sums calculated above and we obtain

$$Q_n^{(l,l+1)}(R) = \frac{1}{4\pi}\sum_l (2l+1)\,l(l+1)f_{nl}^2(R)$$
$$= \frac{4R^2}{3}\left(E_n + \frac{Z}{R}\right)Q_n(R)$$
$$-\frac{2Z}{3}\left[\frac{\phi_{n0}^2(R)}{R} + \frac{1}{2}\,\frac{\mathrm{d}\phi_{n0}^2(R)}{\mathrm{d}R}\right], \qquad (101)$$

$$Q_n^{(\theta,\theta)}(R) = \frac{1}{8\pi R^2}\sum_l (2l+1)\,l(l+1)f_{nl}^2(R)$$
$$= \frac{2}{3}\left(E_n + \frac{Z}{R}\right)Q_n(R) - \frac{Z}{3R^2}\left[\frac{\phi_{n0}^2(R)}{R} + \frac{1}{2}\,\frac{d\phi_{n0}^2(R)}{dR}\right]. \qquad (102)$$

These sums can also be obtained by the expansion of function (96) in a power series of $|\mathbf{r}-\mathbf{R}|$ in the limit $\mathbf{r} \to \mathbf{R}$, but this way is much more complicated.

The sum $Q_n^{(\theta,\theta)}(R)$ defined by formula (102) is shown in Fig. 6 as a function of R in comparison with the sum $Q_n^{(1,1)}(R)$ presented by formula (90). Both the sums are positive for all R. However, the sum $Q_n^{(1,1)}$ decreases stepwise in the region of classically allowed motion, $R \leqslant r_n$, whereas the sum $Q_n^{(\theta,\theta)}(R)$ has no steps. Most other sums also show a peculiar behavior as a function of R [13]. All the sums were calculated both by means of derived quadratic forms of the function ϕ_{n0} and by means of direct summation over l with the use of Coulomb functions f_{nl} [7]. The calculated results coincided every time.

Sums (101) and (102) simplify the investigation of the asymptotics (as $R \to \infty$) of the active-state wave functions (95) and (96) for negative ions with an orbital momentum

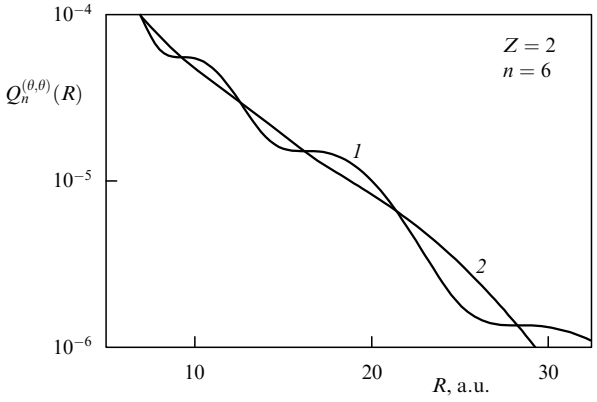

Figure 6. Sums $Q_n(R)$ (curve *1*) and $Q_n^{(\theta,\theta)}$ (curve *2*) as functions of the distance R from the ion $He^{+,*}(n)$ nucleus [equations (90) and (102), respectively].

$L = 1$. The asymptotic limit of the sum $Q_n^{(1,1)}$ equals

$$Q_n^{(1,1)}(R) \to \frac{Z^2}{n^2}\, Q_n(R) \approx \frac{1}{(n!)^2}\,\frac{Z^5}{\pi n^4}\left(\frac{2ZR}{n}\right)^{2n-2}\exp\left(-\frac{2ZR}{n}\right). \quad (103)$$

We can neglect the first terms in square brackets in formulas (95) and (96), because in comparison with other terms they are of order R^{-1} at large internuclear distances R. Then we obtain that as $R \to \infty$ the function $\Psi_n^z(\mathbf{R},\mathbf{r})$ goes over, similar to function $\Psi_n(\mathbf{R},\mathbf{r})$, to the Stark wave function with the maximum dipole moment for a given principal quantum number n, i.e. the limiting expression of the function $\Psi_n^z(\mathbf{R},\mathbf{r})$ is given by formula (85).

The electron dipole moment in the state Ψ_n^z is represented in the following way:

$$d_n^z(R) = -\frac{3n}{4\pi Z Q_n^z(R)}\sum_{l=0}^{n-1} l\sqrt{n^2-l^2}\,\frac{\mathrm{d}f_{n,l}(R)}{\mathrm{d}R}\,\frac{\mathrm{d}f_{n,l-1}(R)}{\mathrm{d}R}. \quad (104)$$

The result of this dipole moment calculation is shown in Fig. 5 together with the calculated result for the integral (86) in the range of internuclear distances $0 \leqslant R \leqslant 20$. It follows from the figure that at large R the dipole moment of the state $\Psi_n^z(\mathbf{R},\mathbf{r})$ is close to the maximum (for $n = 4$ and $Z = 2$) value of $d_n^z = 9$ a.u. However, at $R = 0$ this dipole moment is not equal to zero (see below).

In order to investigate the function $\Psi_n^{x,y}(\mathbf{R},\mathbf{r})$ limit as $R \to \infty$, we should examine the asymptotic limit of the sum $Q_n^{(\theta,\theta)}(R)$ which decreases at large R much more rapidly than the sums $Q_n(R)$ and $Q_n^{(1,1)}(R)$. Only the fifth term in the expansion of expression (102) is nonzero.

The asymptotics of the sum $Q_n^{(\theta,\theta)}(R)$ can be found easily by taking the sum over orbital momentum l, which is present in formula (102) and appears as the definition of the function $Q_n^{(\theta,\theta)}(R)$. Substituting the asymptotics of radial functions $f_{nl}(R)$ [7] into this sum, we arrive at the following result for $R \to \infty$:

$$Q_n^{(\theta,\theta)}(R) \equiv \sum_{l=0}^{n-1}\frac{2l+1}{4\pi}\,\frac{l(l+1)}{2R^2}\,f_{nl}^2(R) \to \frac{2Z^5}{\pi n^6}\,S(n)\left(\frac{2ZR}{n}\right)^{2n-4}\exp\left(-\frac{2ZR}{n}\right), \quad (105)$$

$$S(n) \equiv \sum_{l=0}^{n-1}\frac{(2l+1)\,l(l+1)}{(n+l)!\,(n-l-1)!} = \frac{n^2(n-1)}{(n!)^2}. \quad (106)$$

Now substituting expression (105) into formula (96) we obtain that the functions $\Psi_n^{x,y}$ are transformed in the limit $R \to \infty$ to the wave functions of Stark states with the projection $m = \pm 1$ of an orbital momentum:

$$\Psi_n^{x,y}(\mathbf{R},\mathbf{r}) \to \psi_{n,|m|,n_1}(\mu,\nu,\phi) = Z^{5/2}\,\frac{\sqrt{2(n-1)}}{n^3}\,\rho\,\exp\left(-\frac{Zr}{n}\right) \times F\left(-n+2,2,\frac{Z\mu}{n}\right)\frac{\{\cos\phi,\sin\phi\}}{\sqrt{\pi}}, \quad n,\quad |m|=1,\quad n_1 = n-2, \quad (107)$$

where $\rho = \sqrt{\mu\nu}$ is the distance from the nucleus of the positive ion along the direction perpendicular to the internuclear axis. These Stark states have the maximum dipole moment among states with principal quantum number n and with orbital momentum projection $|m| = 1$:

$$d_{n,|m|=1} = 3n\,\frac{(n-2)}{2Z}.$$

For $Z = 2$ and $n = 4$, the value of this dipole moment runs into $d_{n,|m|=1} = 6$ a.u.

For arbitrary R, the dipole moments corresponding to the $\Psi_n^{x,y}(\mathbf{R},\mathbf{r})$ states are the same and equal to

$$d_n^{x,y}(R) = -\frac{3n}{8\pi Z R^2\, Q_n^{x,y}(R)} \times \sum_{l=0}^{n-1} l(l^2-1)\sqrt{n^2-l^2}\,f_{n,l}(R)f_{n,l-1}(R). \quad (108)$$

The dipole moment $d_n^{x,y}(R)$ is plotted in Fig. 5 as a function of R and has been computed by formula (86) and by sum (108) for $Z = 2$ and $n = 4$. The results of interest coincide and at large R the dipole moment is really equal to 6 a.u.

The presence of dipole moments of excited Rydberg electrons is extremely important for the physics of Rydberg molecules [27]. Vibrational states of such molecules are of the order of $2n^2$ in extent, so that for $n \approx 30$ one obtains 1800 a_0. Rydberg molecules with large electron dipole moments are very sensitive even to relatively weak laser radiation that makes it possible to control the appropriate molecular states with high accuracy [27].

The limiting expressions of sums $Q_n(R)$ as $R \to 0$ are the following:

$$Q_n(0) = \frac{Z^3}{\pi n^3}, \quad Q_n^{(1,1)}(0) = \frac{Z^5(4n^2-1)}{3\pi n^5}, \quad Q_n^{(\theta,\theta)}(0) = \frac{Z^5(n^2-1)}{3\pi n^5}. \quad (109)$$

The wave function of an active state for $L = 0$ is transformed at $R = 0$ to the Coulomb spherical wave function of an S-state:

$$\Psi_n(\mathbf{R}=0,\mathbf{r}) = \psi_{n0}(r) \equiv \frac{1}{\sqrt{4\pi}}\,f_{n0}(r), \quad (110)$$

and functions $\Psi_n^{x,y}$ ($L=1$) for $|m|=1$ are transformed to Coulomb spherical wave functions of P-states:

$$\Psi_n^{x,y}(\mathbf{R}=0,\mathbf{r}) = \sqrt{\frac{3}{4\pi}}\, f_{n,1}(r)\sin\theta\,\{\cos\phi,\sin\phi\}\,. \quad (111)$$

The function $\Psi_n^z(\mathbf{R},\mathbf{r})$ ($L=1$, $m=0$) has a more interesting limit at $R=0$, being represented by the linear combination of the wave functions of S- and P-states:

$$\Psi_n^z(\mathbf{R}=0,\mathbf{r}) = C_0\psi_{n,0}(r) + C_1\psi_{n,1,0}(\mathbf{r}),$$
$$\psi_{n,1,0}(\mathbf{r}) = \sqrt{\frac{3}{4\pi}} f_{n,1}(r)\cos\theta \quad (112)$$

with coefficients

$$C_0 = -\sqrt{\frac{3n^2}{4n^2-1}},\quad C_1 = \sqrt{\frac{n^2-1}{4n^2-1}},\quad C_0^2 + C_1^2 = 1. \quad (113)$$

In the state with the wave function (112), the electron possesses the dipole moment

$$d_n^z(0) = \int z\left|\Psi_n^z(0,\mathbf{r})\right|^2 \mathrm{d}\mathbf{r} = 2C_0C_1\int z\,\psi_{n,0}(r)\,\psi_{n,1,0}(\mathbf{r})\,\mathrm{d}\mathbf{r} = \frac{3n^2(n^2-1)}{Z(4n^2-1)}\,. \quad (114)$$

For $Z=2$ and $n=4$, this dipole moment takes the value $d_n^z(0) = 120/21 = 5.714\ldots$, while the numerical integration yielded $d_{n,z}(0) = 5.712\ldots$ (see Fig. 5, curve *2*).

The wave functions (57) and (58) of passive states constructed in Section 2.3 are orthogonal to the wave functions of active states at any internuclear distance R. Therefore, most likely that these functions are also transformed (as $R\to\infty$) to the wave functions of Stark states. However, this question has not been investigated in detail.

The existence of the above-discussed sums of the Coulomb wave function products signifies that there exist corresponding relationships among confluent hypergeometric functions. These relationships are very complicated and are missing from available reference books [28, 29].

2.5 The distant crossing approach

In the preceding sections, the energy E and internuclear separation R in the $A^- + B^{Z+}$ system were assumed to be independent parameters. The Coulomb Green function, which is the wave function of the outer (or weakly bound) electron, was investigated on the entire half-plane $\{E,R\}$. In this section, we calculate the energy E as a function of the internuclear separation R.

In the zero-order approximation, this electron energy follows the law (12). For internuclear separations $R\sim R_n$ [see formula (25)] close to distant term crossings, where R_n is larger than the size of the corresponding Coulomb orbit for a covalent state, the matrix element taken between the ionic and covalent states is small compared to the difference between the Coulomb terms, viz. Z^2/n^3. In this case, the two-level approximation may be used for the description of an adiabatic wave function:

$$\Phi(\mathbf{R},\mathbf{r}) \approx B(E)\,\Phi_0\big(|\mathbf{R}-\mathbf{r}|\big) + C_n(E)\,\Psi_n(\mathbf{R},\mathbf{r})\,. \quad (115)$$

Within this consideration, the ionic state Φ_0 interacts with the active adiabatic state $\Psi_n(\mathbf{R},\mathbf{r})$ that belongs to only one principal quantum number n.

If the ionic term is close to the covalent term E_n, then in expansions (26), (45) only the coefficient $C_n\simeq 1$ and all other coefficients $C_{n'}$ ($n'\neq n$), are small. Using this property and relations (29) and (47) between the coefficients C_n and the function B, the normalization of the function (115) yields

$$1 = B_n^2(E) + C_n^2(E) = B_n^2(E)\left[1+\frac{\Delta E_n^2(R)}{(E-E_n)^2}\right], \quad (116)$$
$$|E-E_n| \ll |E_n - E_{n\pm1}| \approx \frac{Z}{n^3},$$

where the quantity $\Delta E_n(R)$ for the case $L=0$ takes the form

$$\Delta E_n(R) \equiv 2\pi N_0\sqrt{Q_n(R)}\,,\qquad L=0\,. \quad (117)$$

For negative ions with an orbital momentum $L=1$, the quantity $\Delta E_n(R)$ in formula (116) and in all subsequent formulas should be replaced by $\Delta E_n^{x,y,z}(R)$ equal to

$$\Delta E_n^{x,y,z}(R) \equiv \frac{N_0^{(1)}\sqrt{3\pi}}{\gamma}\sqrt{Q_n^{x,y,z}(R)}\,,\qquad L=1\,. \quad (118)$$

Equalities (117), (118) follow from formulas (27), (46), while the sums $Q_n(R)$ and $Q_n^{x,y,z}(R)$ were calculated in the previous section.

From equality (116) we obtain the relationship for the function $B_n(E)$, and its substitution into Eqns (29) and (47) yields the coefficients $C_n(E)$ and $C_{n'}(E)$ as a function of the energy near crossings:

$$B_n(E) = (E-E_n)\big[(E-E_n)^2 + \Delta E_n^2(R)\big]^{-1/2}, \quad (119)$$

$$C_n(E) = -\Delta E_n(R)\big[(E-E_n)^2 + \Delta E_n^2(R)\big]^{-1/2}, \quad (120)$$

$$C_{n'}(E) = -\Delta E_{n'}(R)\,\frac{E-E_n}{E_n-E_{n'}}\big[(E-E_n)^2 + \Delta E_n^2(R)\big]^{-1/2}. \quad (121)$$

The subscripts n of all the coefficients signify their belonging to the nth avoided crossing: $E\approx E_n$, $n'\neq n$.

Let us write the relations (119)–(121) making use of the zero approximation (12) for the energy. For any n, the difference $E_0(R) - E_n$ can be represented in the form

$$x_n(R) \equiv E_0(R) - E_n = Z\,\frac{R-R_n}{RR_n}\,, \quad (122)$$

which is an exact expression free of any simplifying assumptions. Substituting this finding into Eqns (119)–(121) we derive the coefficients $B_n(R)$, $C_n(R)$, $C_{n'}(R)$ as functions of the internuclear distance R but not the energy:

$$B_n(R) = (-1)^{n-n_{\max}}(R-R_n)\big[(R-R_n)^2 + \Delta R_n^2(R)\big]^{-1/2}, \quad (123)$$

$$C_n(R) = -(-1)^{n-n_{\max}}\,\Delta R_n(R)\big[(R-R_n)^2 + \Delta R_n^2(R)\big]^{-1/2}, \quad (124)$$

$$C_{n'}(R) = -(-1)^{n-n_{\max}}\,\Delta R_{n'}(R)\,\frac{E_0(R)-E_n}{E_n-E_{n'}} \times\big[(R-R_n)^2 + \Delta R_n^2(R)\big]^{-1/2}, \quad (125)$$

where

$$\Delta R_n(R) \equiv \frac{RR_n}{Z}\,\Delta E_n(R)\,. \tag{126}$$

Notice that the quantity $\Delta R_n(R_n) = \Delta E_n(R)/F_n$ at $R = R_n$, where the 'force' $F_n = Z/R_n^2$.

Representing the coefficients B and C as functions of R allows the two-level approximation under consideration to be compared with the exact calculation described in Section 2.1. The function $B(R)$ calculated in the two-level approximation with formula (123) is compared in Fig. 7 with the result of the exact calculation for the collision $H^- + He^{++}$ at $R \sim R_4$. The agreement between the results is very nice, so the two-level approximation proves to be very close to the exact computation. For $R \sim R_5$ and $R \sim R_3$, the two-level approximation is equally close to the exact evaluation.

The coefficients B and C in formulas (119)–(121) are the functions of energy. To determine the system's energy as a function of the internuclear separation R, we may take advantage of the fact that closer inspection of the two-level approximation enables us to consider the adiabatic wave functions $\psi_{1,2}$ as linear combinations of the wave functions $\phi_{1,2}$ defined in the zero-order approximation [7, 33]:

$$\psi_1 = a\phi_1 + b\phi_2\,, \qquad \psi_2 = -b\phi_1 + a\phi_2\,, \tag{127}$$
$$a = \left[\frac{\sqrt{x^2+\Delta^2}+x}{2\sqrt{x^2+\Delta^2}}\right]^{1/2}, \qquad b = \left[\frac{\sqrt{x^2+\Delta^2}-x}{2\sqrt{x^2+\Delta^2}}\right]^{1/2},$$

where the difference between the diagonal matrix elements x and twice the nondiagonal matrix element Δ is written in our notation as

$$x \equiv E_1^0 + V_{11} - E_2^0 - V_{22} \approx E_0(R) - E_n\,, \qquad \Delta \equiv 2|V_{0n}|\,.$$

The equality $B_n = C_n = 1/\sqrt{2}$ with $E - E_n = \Delta E_n(R)$ follows from formulas (119) and (120). In turn, relationship (127) shows that these coefficients correspond to a minimum energy difference between two avoided crossing terms, when $x = 0$. Thus, for the $A^- + B^{Z+}$ system under study, we can write down an expression for the nondiagonal matrix element in the form

$$V_{0n} = \langle \Phi_0 | V | \Psi_n \rangle = \Delta E_n(R)\,, \tag{128}$$

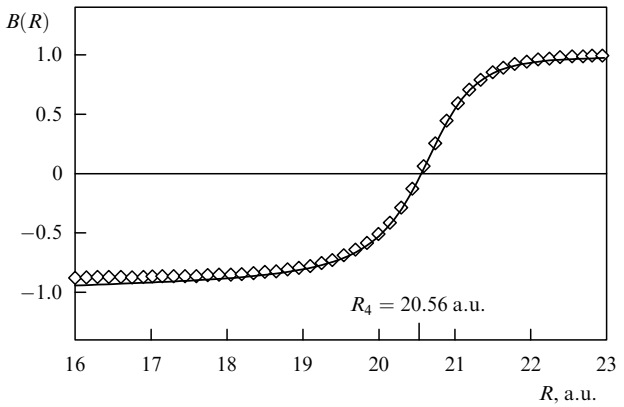

Figure 7. Function $B(R)$ versus the internuclear distance R for the $H^- + He^{++}$ system near the crossing of the ionic term with the covalent $n = 4$-term: solid line — the exact numerical calculation with formulas (22), (24); diamonds — the distant crossing approach resulted in formula (123).

and the expression for the energies of the two avoided crossing terms as

$$E_\pm(R) - E_n = \frac{1}{2}\left[E_0(R) - E_n \pm \left((E_0(R) - E_n)^2 + 4\Delta E_n^2(R)\right)^{1/2}\right], \tag{129}$$

because the diagonal matrix element for the ionic state is

$$\hat{H}_{00} = E_0(R) = \varepsilon_0 - \frac{Z}{R}\,, \tag{130}$$

and because the shifts of covalent terms may be neglected by assuming that $\hat{H}_{nn} \approx E_n$. Substituting the expressions (129) for energy into Eqns (119) and (120), we arrive at relationships (127).

In equation (129) for the energy levels, the energy terms $\Delta E_n(R)$ are present. According to relations (117), (118) these terms are expressed through the sums of Coulomb wave function products $Q_n, Q_n^{(1,1)}, Q_n^{(2,2)}$ and $Q_n^{(\theta,\theta)}$ calculated in the preceding section. These sums were shown in Fig. 3. As follows from these figures, the $Q_n, Q_n^{(1,1)}, Q_n^{(2,2)}$ and $Q_n^{(\theta,\theta)}$ sums, and, hence, the nondiagonal matrix elements V_{0n} are nonzero at all finite internuclear separations R for negative ions with any orbital momentum L. Therefore, within the limits of our approximation we have avoided crossings but not direct crossings of energy levels. The energy splittings at avoided crossings are equal to $2\Delta E_n(R_n) \neq 0$. In Tables 1 and 2, the values of these splittings are quoted for the systems $H^- + H^+$ and $H^- + He^{++}$.

Table 1. Orbit sizes r_n, avoided crossing positions R_n and energy splittings $\delta E_n(R_n) = 2\Delta E_n(R_n)$ for the $H^- + H^+$ system.

n	r_n, a.u.	R_n, a.u.	$\delta E_n(R_n)$, a.u.
1	2.0	2.117	1.652^{-1}
2	8.0	10.279	1.876^{-2}
3	18.0	35.921	2.318^{-4}
4	32.0	283.005	7.123^{-27}

Table 2. Orbit sizes r_n, avoided crossing positions R_n and energy splittings $\delta E_n(R_n) = 2\Delta E_n(R_n)$ for the $H^- + He^{++}$ system.

n	r_n, a.u.	R_n, a.u.	$\delta E_n(R_n)$, a.u.
1	1.0	1.01	5.108^{-1}
2	4.0	4.23	1.059^{-1}
3	9.0	10.28	3.126^{-2}
4	16.0	20.56	7.429^{-3}
5	25.0	38.25	7.179^{-4}
6	36.0	71.84	5.089^{-6}
7	49.0	152.67	3.556^{-12}
8	64.0	566.01	5.148^{-50}

In the δ-potential approach, the energy levels of the system $A^- + B^+$ for the negative ion A^- with zero angular momentum ($L = 0$) may be found from the solution of the transcendental equation with the logarithmic derivative of the Coulomb Green function [3]:

$$\frac{\partial}{\partial|\mathbf{r}-\mathbf{R}|}\ln G(|\mathbf{r}-\mathbf{R}|) \equiv \frac{2\Gamma(1-Z\nu)}{\nu}\left[W'_+(\tau)\,M'(\tau) + \left(-\frac{1}{4} + \frac{Z\nu^2}{2R}\right)W_+(\tau)\,M(\tau)\right]_{\tau=2R\nu} = -\gamma\,. \tag{131}$$

In Fig. 8, the energy level behavior near the avoided crossing with a covalent level $n = 4$ is illustrated for the

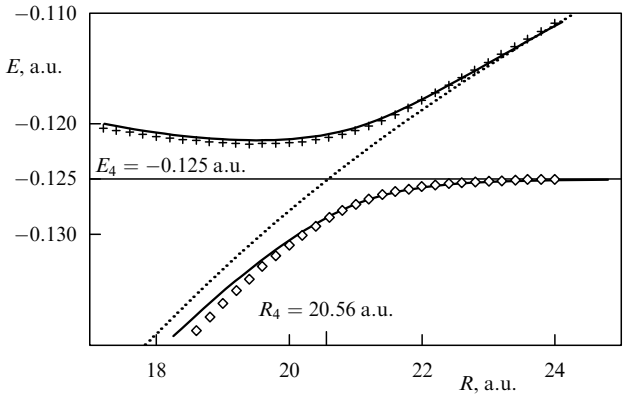

Figure 8. Energy levels of the $H^- + He^{++}$ system near the avoided crossing of the ionic energy level with the covalent $n = 4$-level. Energies are shown as a function of the internuclear distance R. The dotted line is the ionic energy in a zero approximation: $E_0(R) = \varepsilon_0 - Z/R$, defined by equation (12); solid lines — the results of the solution of the transcendent equation (131) with the logarithmic derivative of the Coulomb Green function; crosses and diamonds — the results of the distant crossing approach introduced by formula (129), produced with the use of expression (117) for $\Delta E_n(R)$ and expression (77) for the sum $Q_n(R)$.

system $H^- + He^{++}$ with $R_4 = 20.56a_0$. The results (solid lines) obtained using the logarithmic derivative (131) are very close to those (crosses and diamonds) found in the distant crossing approach (129).

Thus, the procedure drawn for normalizing the Coulomb Green function as the wave function and analyzing the results allows us to calculate the nondiagonal matrix elements and to determine the behavior of the terms for each crossing, i.e. this procedure allows the behavior of the $A^- + B^+$ system to be completely described.

For calculation of the electron capture cross sections in collisions (1) and (2), the system of adiabatic equations [34]

$$\frac{\mathrm{d}a_{nlm}(t)}{\mathrm{d}t} = \sum_{n',l',m'} a_{n'l'm'}(t)\left(\frac{\mathrm{d}}{\mathrm{d}t}\right)^{nlm}_{n'l'm'} \times \exp\left(\int^t E_n^{n+1}\big(R(t')\big)\,\mathrm{d}t'\right) \tag{132}$$

was solved in Ref. [8]. In these equations, the adiabatic energy levels are defined as

$$E_n^{n+1}(R) = \frac{1}{2}\begin{cases} E_0(R) + E_{n+1} - D_{n+1}(R)\,, & R \geqslant R_n^{n+1}\,, \\ E_0(R) + E_n + D_n(R)\,, & R \leqslant R_n^{n+1}\,, \end{cases} \tag{133}$$

$$D_n(R) \equiv \big(x_n^2(R) + 4\Delta E_n^2(R)\big)^{1/2}, \quad R_n^{n+1} \equiv \frac{1}{2}(R_n + R_{n+1})\,,$$

and $x_n(R)$ is specified in formula (122). At $R < R_n$, the energy $E_n^{n+1}(R)$ is close to the Coulomb energy E_n, and at $R > R_{n+1}$ to the energy E_{n+1}. In the range between avoided crossings, viz. at $R_n < R < R_{n+1}$, this energy is close to the zero-approximation ionic energy $E_0(R)$.

The system of adiabatic wave functions was constructed in the form [8]

$$\Phi_n^{n+1}(\mathbf{R},\mathbf{r}) = \begin{cases} C_{n+1}^-(R)\,\Phi_0\big(|\mathbf{R}-\mathbf{r}|\big) + C_{n+1}^+(R)\,\Psi_{n+1}(\mathbf{R},\mathbf{r})\,, & R \geqslant R_n^{n+1}\,, \\ C_n^+(R)\,\Phi_0\big(|\mathbf{R}-\mathbf{r}|\big) - C_n^-(R)\,\Psi_n(\mathbf{R},\mathbf{r}), & R \leqslant R_n^{n+1}\,, \end{cases} \tag{134}$$

where the coefficients $C_n^{\pm}$ and the function $B_n^{n+1}(R)$ are determined in the following way:

$$C_n^{\pm}(R) = \left(\frac{D_n(R) \pm x_n(R)}{2D_n(R)}\right)^{1/2},$$

$$B_n^{n+1}(R) = \begin{cases} C_{n+1}^-(R)\,, & R \geqslant R_n^{n+1}\,, \\ C_n^+(R)\,, & R \leqslant R_n^{n+1}\,. \end{cases} \tag{135}$$

The coefficients $C_{n,n'}^{\pm}(R)$ describing the contributions to the function Φ_n^{n+1} of the states with principal quantum numbers $n' \neq n$ are

$$C_{n,n'}^{\pm}(R) = \mp\frac{\Delta E_{n'}(R_n)}{E_n - E_{n'}}\,C_n^{\pm}(R)\,. \tag{136}$$

At $R < R_n$, the function Φ_n^{n+1} is close to the function Ψ_n, because in this region $|C_n^-| \sim 1$ and $C_n^+ \sim 0$. At the avoided crossing $R \approx R_n$, the function Φ_n^{n+1} is a linear combination of the functions Ψ_n and Φ_0. At the next avoided crossing $R \approx R_{n+1}$, this function is a linear combination of the functions Φ_0 and Ψ_{n+1}. In the region between crossings, viz. at $R_n < R < R_{n+1}$, the function Φ_n^{n+1} is close to the unperturbed wave function Φ_0 of the negative ion, in so far as the amplitude $B_n^{n+1}(R)$ is close to unity, and all $C_n^{\pm}$ are small. At $R > R_{n+1}$, the function Φ_n^{n+1} is close to Ψ_{n+1}, because here one finds $|C_{n+1}^+| \sim 1$ and $C_{n+1}^- \sim 0$.

In the coordinate system the z-axis of which is perpendicular to the collision plane, only the absolute value of an interionic distance R and azimuthal angle ϕ_R of the vector $\mathbf{R}$ depend on time. The polar angle is unchanged and equal to $\theta_R = \pi/2$. Therefore, the time-dependent derivative can be written in the form

$$\frac{\mathrm{d}}{\mathrm{d}t} = \dot{\phi}_R\,\frac{\mathrm{d}}{\mathrm{d}\phi_R} + \dot{R}\,\frac{\mathrm{d}}{\mathrm{d}R}\,.$$

The adiabatic matrix elements between two avoided crossing states exhibit only radial coupling. They only depend on the derivatives with respect to R and are equal to

$$V_{n-1}^n\big(R(t)\big) \equiv \left(\frac{\mathrm{d}}{\mathrm{d}R}\right)^{n,n+1}_{n-1,n} \equiv \int \Phi_{n-1}^n(\mathbf{R},\mathbf{r})\,\frac{\mathrm{d}\Phi_n^{n+1}(\mathbf{R},\mathbf{r})}{\mathrm{d}t}\,\mathrm{d}\mathbf{r} = C_n^-\,\frac{\mathrm{d}C_n^+}{\mathrm{d}R} - C_n^+\,\frac{\mathrm{d}C_n^-}{\mathrm{d}R} = \frac{Z}{R^2}\,\frac{2\pi N_0}{\sqrt{Q_n(R)}}\,\frac{Q_n(R) - x_n(R)R^2Q_n'(R)/2R}{x_n^2 + 4(2\pi N_0)^2\,Q_n(R)}\,. \tag{137}$$

These matrix elements are nonzero in narrow ranges ΔR_n near the points R_n of avoided crossings, and their absolute values are large at $R = R_n$:

$$V_{n-1,\max}^n\big(R(t)\big) = \left(\frac{\mathrm{d}}{\mathrm{d}R}\right)^{n,n+1}_{n-1,n}\Bigg|_{R=R_n} = \frac{Z}{4R_n^2\,\Delta E_n(R_n)}\,. \tag{138}$$

Near the nth crossing, the matrix elements taken between the active crossing states and the other active states $\Psi_{n'}$ that are not involved in the nth crossing, i.e. for $n' \neq n$, are also at a maximum. Using the coefficients $C_{n'}$ defined by formula (121) we obtain

$$U_{n-1}^{n'}\big(R(t)\big) = \left(\frac{\mathrm{d}}{\mathrm{d}R}\right)^{n'}_{n-1,n} = \frac{\mathrm{d}C_{n,n'}^-}{\mathrm{d}R} = -\frac{\Delta E_{n'}(R_n)}{E_n - E_{n'}}\,\frac{\mathrm{d}C_n^-}{\mathrm{d}R}\,,$$

$$U_n^{n'}\big(R(t)\big) = \left(\frac{\mathrm{d}}{\mathrm{d}R}\right)^{n'}_{n,n+1} = \frac{\mathrm{d}C_{n,n'}^+}{\mathrm{d}R} = \frac{\Delta E_{n'}(R_n)}{E_n - E_{n'}}\,\frac{\mathrm{d}C_n^+}{\mathrm{d}R}\,, \tag{139}$$

$$\frac{\mathrm{d}C_n^{\pm}(R)}{\mathrm{d}R} = \pm 4\sqrt{2}\pi^2 N_0^2 \frac{Z}{R^2} \frac{Q_n(R) - x_n(R)\, R^2\, Q_n'(R)/2R}{D_n^{5/2}(R)\big(D_n(R) \pm x_n(R)\big)^{1/2}}. \quad (140)$$

The maximum absolute values of these matrix elements are reached at $R = R_n$:

$$\left.\frac{\mathrm{d}C_{n,n'}^{\pm}(R)}{\mathrm{d}R}\right|_{R=R_n} = \pm \frac{\Delta E_{n'}(R_n)}{\sqrt{2}(E_n - E_{n'})} \frac{Z}{4R_n^2 \Delta E_n(R_n)}. \quad (141)$$

These values are a factor of $\Delta E_{n'}(R_n)/\big(\sqrt{2}(E_n - E_{n'})\big)$ smaller than the maximum values (138) of matrix elements (137) between the wave functions of active states for a given n. The matrix elements (137) and (139) are depicted in Figs 9 and 10.

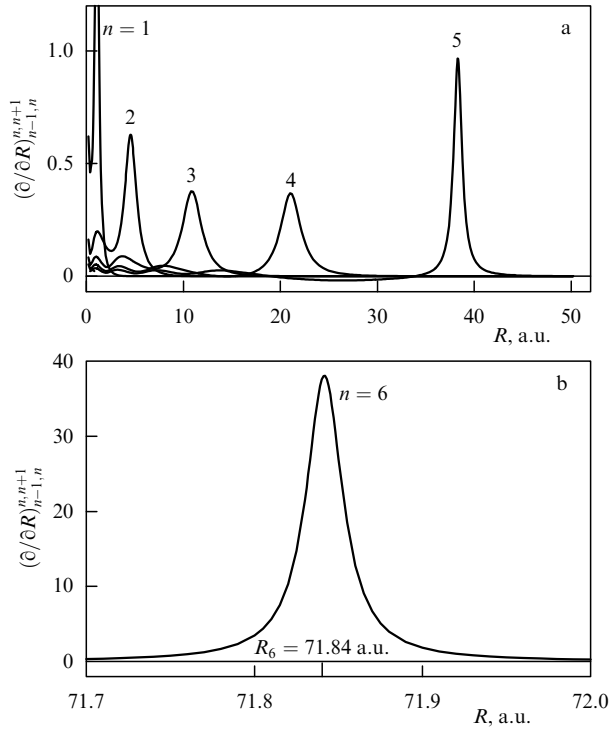

Figure 9. Adiabatic radial matrix elements $(\partial/\partial R)_{n-1,n}^{n,n+1}$ (137) between two avoided crossing states for the $H^- + He^{++}$ system with $L = 0$ as a function of internuclear distance R for principal quantum numbers of avoided crossings $n = 1 - 5$ (a), and $n = 6$ (b).

For negative ions with an orbital momentum $L = 1$, the sum $Q_n(R)$ in formulas (137)–(141) should be replaced by the sum $Q_n^{(1,1)}$ or by the sum $Q_n^{(\theta,\theta)}(R)$. Similarly, the energy splitting $\Delta E_n(R)$ should be replaced by $\Delta E_n^{x,y,z}(R)$.

In Fig. 11, the total cross section of the ion–ion recombination $H^- + He^{++} = H + He^+(n)$ is shown. It has been derived by solving the system of close coupling equations (132) including the covalent states with principal quantum numbers $1 \leqslant n \leqslant 10$ (385 states) [8]. The results of this calculation are compared with experimental results [35–38] and with those of variational calculations [35, 39]. We see that the calculated results [8] coincide with the measurement data [35].

At the same time, the experimental cross section from paper [35] and the cross section calculated in paper [8] are in

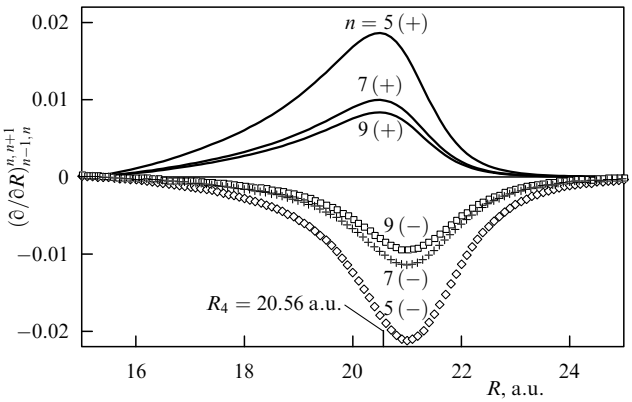

Figure 10. Adiabatic radial matrix elements $(\partial/\partial R)_{n-1,n}^{n,n+1}$ (139) between two avoided crossing states indicated by '+' and '–' for the $H^- + He^{++}$ system with $L = 0$, $n = 4$ and active states with principal quantum numbers $n' = 5, 7, 9$ ($n' \neq n$).

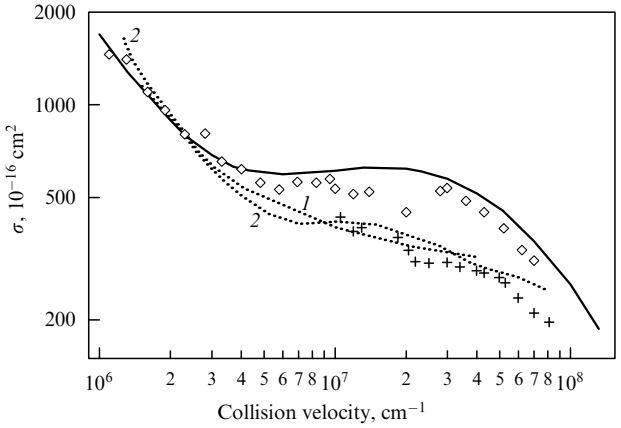

Figure 11. Total electron capture cross section in the collision $H^- + He^{++} = H + He^+(n)$ as a function of collision velocity. Experimental results: diamonds — from Ref. [35], and crosses — from Ref. [36]. Theory: solid line — calculated results [8]; dotted curve *1* — results of variational calculations [39], and dotted curve *2* — results of variational calculations [35].

1.3–1.6 times larger than the cross sections found by measurement [36] and in variational calculations [35, 39]. This difference is explained as follows. In calculations [35, 39] only the states $n = 2-5$ were taken into account. In paper [8] it was found that the maximum populated states are states with principal quantum numbers $n = 4-6$ and this finding is in agreement with the variational calculations [35, 39]. However, taking into account the states $n = 7-10$ is also necessary.

The population of each of these highly excited states is significantly smaller than the populations of $n = 4-6$-states but their contribution to the total cross section measures about 50–60%. An appreciable population of the states $n = 7-10$ occurs at the moment when the system passes crossings with $n = 4, 5$ levels. The coupling between states with $n = 7-10$ and $n = 4, 5$ is given by matrix elements (139). The same effect takes place at the collision $H^- + A^{3+}$ [40–42]. It should be emphasized that in paper [43] the electron capture (1) has been interpreted as the tunneling electron transition through the potential barrier from a negative ion to a positive ion.

3. Collisions of two negative ions

The electron detachment processes proceeding at the collision of two negative ions are of considerable interest in connection with the problem of nuclear fusion plasma heating by neutral atomic hydrogen beams. It is convenient to generate the beams of fast neutral atoms by accelerating and neutralizing the negative ions in view of the relatively large cross section of their neutralization in targets. However, the collisions of negative ions inside high-intensity beams, which occur due to the spread in their velocities, effectively suppress the intensity of such beams. The electron detachment in the collision of two atomic hydrogen negative ions, $H^- + H^-$, was studied earlier both experimentally [44, 45] and theoretically [46–52].

Three processes of weakly bound electron detachment are possible in a collision of two negative ions:

$$\begin{aligned} A^- + B^- &= A + B^- + e\,, && \text{(A)}\\ &= A^- + B + e\,, && \text{(B)}\\ &= A + B + 2e\,, && \text{(AB)} \end{aligned}$$

whose probabilities strongly compete with one another. Reactions (A), (B), and (AB) were investigated in work [46] for the following three collision pairs: $H^- + H^-$, $H^- + Cs^-$ and $Cs^- + Cs^-$.

The two-negative-ion collision is similar in some details to the negative ion collision with a negatively charged classical point particle: with the electron regarded as a classical particle [53, 54], and with the antiproton [55, 56]. However, essential discrepancies between these collisions also exist. If the system of a negative ion and antiproton can be considered as a one-electron one, then the two-negative-ion system is a two-electron one.

The adiabatic wave function of the weakly bound electron in the negative ion–antiproton system is given by formula (11) with the Coulomb Green function for the repulsion field. But for the two-negative-ion system, formula (11) is not applicable. The two-negative-ion wave function can be written as a product of the two Coulomb Green functions. However, this representation is rather complex and we do not apply it.

The cross sections of reactions (A), (B) and (AB) are sufficiently large and we shall take into account the transitions of only weakly bound electrons. Then the complete set of two-negative-ion states is expressed as follows

$$\psi_a^{(-)}(\mathbf{r}_{1a})\,\psi_b^{(-)}(\mathbf{r}_{2b})\,\exp\bigl(-\mathrm{i}(\varepsilon_a+\varepsilon_b)t\bigr), \tag{142}$$

$$\psi_a^{\varepsilon}(\mathbf{r}_{1a})\,\psi_b^{(-)}(\mathbf{r}_{2b})\,\exp\bigl(-\mathrm{i}(\varepsilon_b+\varepsilon)t\bigr)\,, \tag{143}$$

$$\psi_a^{(-)}(\mathbf{r}_{1a})\,\psi_b^{\varepsilon}(\mathbf{r}_{2b})\,\exp\bigl(-\mathrm{i}(\varepsilon_a+\varepsilon)t\bigr)\,, \tag{144}$$

$$\psi_a^{\varepsilon}(\mathbf{r}_{1a})\,\psi_b^{\varepsilon'}(\mathbf{r}_{2b})\,\exp\bigl(-\mathrm{i}(\varepsilon+\varepsilon')t\bigr)\,, \tag{145}$$

where $\psi_{a,b}^{(-)}$ are the wave functions of weakly bound electrons, and $\psi_{a,b}^{\varepsilon}$ are the wave functions of the system involving a neutral atom and an electron in the continuum with an energy ε. Expression (142) relates to the wave function of the system formed by two negative ions, i.e. the wave function of the initial state; expressions (143) and (144) describe the state in which the electron of one of the ions, A or B, is detached and resides in the continuum, while expression (145) identifies the state with two detached electrons.

3.1 Small collision velocities. Auger decays

If the distance between two negative ions decreases slowly, then the total binding energy of weakly bound electrons goes up to the continuum as a result of the interelectron repulsion. This energy crosses the continuum boundary at very large internuclear distance R because the negative ion binding energy is small. At distances smaller than the crossing distance $R_{a,b}$, a few Auger decay channels become open. One or two weakly bound electrons are detached as a result of these Auger decays [46, 47].

At large R, the interelectron repulsion can be expanded in a power series of the inverse degrees of R:

$$\begin{aligned} \frac{1}{|\mathbf{r}_1-\mathbf{r}_2|} \approx \frac{1}{R} &+ \frac{z_{1a}}{R^2} + \frac{3z_{1a}^2 - r_{1a}^2}{2R^3} + \frac{r_{1a}z_{1a}(5z_{1a}-3r_{1a})}{2R^4}\\ &+ \ldots + \frac{z_{2b}}{R^2} + \frac{3z_{2b}^2 - r_{2b}^2}{2R^3} - \frac{r_{2b}z_{2b}(5z_{2b}-3r_{2b})}{2R^4}\\ &+ \ldots + W(\mathbf{r}_{1a},\mathbf{r}_{2b}) + \ldots\,, \quad r_{1a},\, r_{2b} \ll R\,, \end{aligned} \tag{146}$$

where $\mathbf{r}_1$, $\mathbf{r}_2$ are the radius vectors of electrons 1 and 2 in an arbitrary coordinate system, and $\mathbf{r}_{1a}$, $\mathbf{r}_{2b}$ are the vectors of electrons 1 and 2 positioned relative to atomic a and b nuclei, respectively.

The correlation term $W(\mathbf{r}_{1a},\mathbf{r}_{2b})$ is the function of the product of the coordinates of both electrons:

$$W(\mathbf{r}_{1a},\mathbf{r}_{2b}) = \frac{\mathbf{r}_{1a}\mathbf{r}_{2b} - 3z_{1a}z_{2b}}{R^3} + \ldots\,, \tag{147}$$

while the remaining terms in expression (146) depend on the coordinates of only one of the electrons. Then the expansion (146) can be written down as

$$\frac{1}{r_{12}} = -\frac{1}{R} + \frac{1}{|\mathbf{R}-\mathbf{r}_{1a}|} + \frac{1}{|\mathbf{R}+\mathbf{r}_{2b}|} + W(\mathbf{r}_{1a},\mathbf{r}_{2b})\,, \tag{148}$$

$r_{1a}, r_{2b} \ll R$.

Using the last relation we can write the wave equations for weakly bound electrons in the form

$$\left(-\frac{\Delta_1}{2} + U_a(r_{1a}) + \frac{1}{|\mathbf{R}-\mathbf{r}_{1a}|} - \frac{1}{R} - E_a(R)\right)\psi_a^{(-)}(\mathbf{r}_{1a}) = 0\,, \tag{149}$$

$$\left(-\frac{\Delta_2}{2} + U_b(r_{2b}) + \frac{1}{|\mathbf{R}+\mathbf{r}_{2b}|} - E_b(R)\right)\psi_b^{(-)}(\mathbf{r}_{2b}) = 0, \tag{150}$$

where $U_{a,b}(r)$ are the interaction potentials of the weakly bound electrons a and b with their own atomic cores. The energies of these electrons are described by the following expressions:

$$E_a(R) \approx \varepsilon_a - \frac{\alpha_a}{2R^4} + \ldots\,, \quad E_b(R) \approx \varepsilon_b + \frac{1}{R} - \frac{\alpha_b}{2R^4} + \ldots\,, \tag{151}$$

where $\varepsilon_{a,b}$ are the unperturbed binding energies of negative ions, and $\alpha_{a,b}$ are their polarizibilities. For large internuclear distances R, viz.

$$R > \frac{1}{\gamma}\,, \tag{152}$$

the polarization terms in formula (147) can be neglected and then the total energy of the two negative ions equals

$$E(R) = E_a(R) + E_b(R) = \varepsilon_a + \varepsilon_b + \frac{1}{R}\,. \tag{153}$$

Formally, equations (149) and (150) are independent of one another. In reality, however, the negative ions are not independent in our approach. Indeed, the term $-1/R$ in equations (149) and (150) can be attributed either to an electron a or to electron b. We should consider both the system of equations (149), (150) and the system with permuted subscripts: $a \leftrightarrow b$, because the electrons are indistinguishable. With the use of a many-electron wave function which is symmetrized over electron permutations, this system property is taken into account automatically. Subsequently, we shall use directly the representations (149), (150), whereas the alternative representation $a \leftrightarrow b$ will be taken into account by analogy.

Equation (150) describes the negative ion b placed in the field of a classical negatively charged point particle (for example, an antiproton $\bar{\mathrm{p}}$). If $R \leqslant R_b \equiv 1/|\varepsilon_b|$, then the energy of an electron b is in the continuum ($E_b > 0$) and electron b can tunnel through the potential barrier into the continuum. At $R < R_a \equiv 1/\varepsilon_a$, the same situation occurs for electron a. The rate of through-barrier tunneling, Γ_{sq} (the subscript 'sq' marks the abbreviated form of a squeezing out), was calculated in Ref. [53] and it takes the form

$$\Gamma_{\mathrm{sq},(a,b)}(R) = \frac{B_{a,b}^2}{2\gamma_{a,b}R^2}\exp\left[-\frac{4}{\gamma_{a,b}}\,y f(y)\right], \tag{154}$$

$$f(y) \equiv \frac{\arcsin\sqrt{y}}{\sqrt{y(1-y)}} - 1\,, \quad y \equiv \frac{R}{R_{a,b}} \leqslant 1\,, \quad R_{a,b} \equiv \frac{1}{|\varepsilon_{a,b}|}\,.$$

The decay rate $\Gamma_{\mathrm{sq},(a,b)}(R) \equiv 0$ at $R \geqslant R_{a,b}$, because at these internuclear distances the energy of the tunneling electron is negative [$E_{a,b}(R) < 0$] and the tunneling itself is forbidden. For the collision $\mathrm{H}^- + \mathrm{H}^-$, we have $R_a = R_b = 36\,a_0$. In paper [47], the probability of squeezing out was calculated with the use of the Coulomb Green function for the case of repulsion and the same result was obtained for the decay rate, viz. expression (154).

If the electron a (or b) is tunneling at $R \leqslant R_{a,b}$, then the electron b (or a) cannot tunnel to the continuum, because in the system $\mathrm{A} + \mathrm{B}^-$ (as in the system $\mathrm{A}^- + \mathrm{B}$) there is no Coulomb interelectron repulsion. The simultaneous tunneling of both electrons is also impossible. Thus, in a two-negative-ion collision, several processes of electron detachment are in cut-throat competition. This very competition is the origin of the distinguishing difference between the two-negative-ion collision and the collision of one negative ion with a classical negatively charged point particle, for example, with an antiproton.

The following expression for the wave function of an unperturbed negative ion [9, 10, 57]:

$$\psi_0^{(-)}(r) = B(\gamma,\beta)\sqrt{\frac{\gamma}{2\pi}}\,\frac{\exp(-\gamma r) - \exp(-\beta r)}{r}\,, \tag{155}$$

$$B(\gamma,\beta) = \frac{(1+\gamma/\beta)^{1/2}}{1-\gamma/\beta}\,,$$

where $\varepsilon = -\gamma^2/2$, was used in the calculation of the electron tunneling probability. The binding energies of negative ions H^- and Cs^- are equal to $\varepsilon_{\mathrm{H}^-} = -0.75421$ eV ($\gamma_{\mathrm{H}^-} = 0.23544$) and $\varepsilon_{\mathrm{Cs}^-} = -0.4716$ eV ($\gamma_{\mathrm{Cs}^-} = 0.1862$), respectively [58].

In papers [9, 10], the wave equation, to which the function (155) satisfies, was considered. The potential energy in this equation was fitted to the static potential of neutral atomic hydrogen in the ground state and the result was obtained for the ion H^-: $\beta_{\mathrm{H}^-} = 2.66$. Then, with the use of equation (155), we found the value of the coefficient B equal to 1.145. This finding is very close to the value $B = 1.183$ which was obtained in book [57] by utilizing the Chandrasekhar wave function [59] of the ion H^-. For Cs^- it was obtained by the method developed in works [9, 10]: $\beta_{\mathrm{Cs}^-} = 1.45$ (see also Ref. [60]) and $B_{\mathrm{Cs}^-} = 1.22$.

If the electron b possesses an excess energy $1/R$, then this electron can transfer the excess energy to the electron a which will be detached at $R \leqslant R_a$. Electron b in this case remains in the bound state so that this process is a one-electron Auger decay. The rate of this decay is determined by the matrix element $W(\mathbf{r}_{1a}, \mathbf{r}_{2b})$ of the correlation interaction. If we calculate this matrix element using the unperturbed wave function (155) of the electron b, this matrix element comes to zero.

Actually, the state of the electron b is perturbed by the interelectron repulsion before the decay and its wave function appears to be polarized and equal to [46]

$$\psi_b^{(-)} = \psi_{b0}^{(-)}(r_{2b})\left[1 - \frac{r_{2b}^2\cos\theta}{2\gamma_b R^2} + O\left(\frac{r_{2b}^3}{R^3}\right)\right]. \tag{156}$$

The wave function of electron b in the continuum assumes the form [46]

$$\psi_b^{\varepsilon}(\mathbf{r}) = \sqrt{\frac{2}{\pi k}}\,\frac{1}{r}\left(\frac{\sin(kr)}{kr} - \cos(kr)\right)$$
$$\times\sqrt{\frac{3}{4\pi}}\left\{\cos\theta,\ \sin\theta\cos\varphi,\ \sin\theta\sin\varphi\right\} \tag{157}$$

with three components of the angular function: $\cos\theta, \sin\theta\cos\varphi$ and $\sin\theta\sin\varphi$. The z-axis of the coordinate system introduced is perpendicular here to the collision plane.

After the calculation of the matrix element we obtain the rate Γ_{1ab} of the one-electron Auger decay [46]:

$$\Gamma_{1,ab}(R) = 2\pi|W_{if}|^2 = \frac{\gamma_a^8 B_a^2 B_b^4}{6\sqrt{2}}\left(\frac{\gamma_a}{\gamma_b}\right)^4\,\frac{(1-x)^{3/2}}{(2x)^{15/2}}\,, \tag{158}$$

$$x \equiv \frac{R}{R_a} < 1$$

with the detachment of an electron a from the negative ion A^- by the negative ion B^-. Similarly, the rate Γ_{1ab} of the one-electron Auger decay with the detachment of an electron from the negative ion B^- by the negative ion A^- is given by [46]

$$\Gamma_{1,ba}(R) = \frac{\gamma_b^8 B_a^4 B_b^2}{6\sqrt{2}}\left(\frac{\gamma_b}{\gamma_a}\right)^4\,\frac{(1-y)^{3/2}}{(2y)^{15/2}}\,, \tag{159}$$

$$y \equiv \frac{R}{R_b} < 1\,, \qquad R_b \equiv \frac{1}{|\varepsilon_b|}\,.$$

If the internuclear distance $R \leqslant R_{ab} \equiv |\varepsilon_a + \varepsilon_b|^{-1}$ ($R_{ab} = 18a_0$ for the collision $\mathrm{H}^- + \mathrm{H}^-$), then two-electron

Auger decay becomes possible. The rate $\Gamma_{ab}(R)$ of the two-electron Auger decay can be calculated using the unperturbed wave functions of the initial state for the system of colliding negative ions and of their states in continuum (157). The electron momenta after Auger decay are confined within some limits set by the energy conservation law:

$$k_a^2 + k_b^2 = 2\left(\frac{1}{R} - |\varepsilon_a + \varepsilon_b|\right).$$

The total rate of the two-electron Auger decay is described as follows [46]

$$\Gamma_{ab}(R) = \frac{2^{10}\gamma_a\gamma_b B_a^2 B_b^2}{3\pi R_{ab}^2}\,\frac{(1-x)^4}{x^2}\int_0^1 \frac{(1-t^2)^{3/2}}{\left[1-(1-x)^2t^2\right]^4}\,\mathrm{d}t,$$

$$R_{ab} \equiv \frac{1}{|\varepsilon_a + \varepsilon_b|}\,, \qquad x \equiv \frac{R}{R_{ab}} < 1\,. \tag{160}$$

The rates of all Auger decays are shown in Fig. 12 as a function of internuclear distance R for the collision $H^- + Cs^-$. The squeezing out rate $\Gamma_{sq}(R)$ has a maximum value in the range of distances $2-3 \leqslant R \leqslant 35$ which make the main contribution to the one-electron detachment cross section at not very low energies. However, the rate of squeezing out exponentially decreases when the negative ions are parted. At distances $R > 35$, the squeezing out rate becomes smaller than the rate of one-electron decay Γ_1 which is the power function of R. Therefore, at a small collision energy the one-electron detachment is determined by the one-electron Auger decay [46]. As a result, the energy dependence of the one-electron detachment cross section essentially changes near the threshold [46]. This effect takes place for all investigated collisions $H^- + H^-$, $H^- + Cs^-$ and $Cs^- + Cs^-$ [46].

The initial state of the two-negative-ion system $A^- + B^-$ decays through five different channels with the formation of three different final states: (A), (B) and (AB). The probabilities of such a decay must be calculated using a multichannel scheme. Let $P_0(\varrho, t)$ be the probability of finding the system in the initial state at the instant of time t for a collision with the impact parameter ϱ, and $\Gamma_{\mathrm{tot}}\big(R(t)\big)$ be the total probability of the decay via all channels. These quantities are connected through the relation

$$P_0(\varrho, t) = \exp\left[-\int_{-\infty}^{t} \Gamma_{\mathrm{tot}}\big(R(t')\big)\,\mathrm{d}t'\right]. \tag{161}$$

The probability of decay through the ith channel is given by expressions

$$P_i(\varrho, t) = \int_{-\infty}^{t} P_0(\varrho, t')\,\Gamma_i\big(R(t')\big)\,\mathrm{d}t'$$

$$= \int_{-\infty}^{t} \Gamma_i\big(R(t')\big)\,\exp\left[-\int_{-\infty}^{t'} \Gamma_{\mathrm{tot}}\big(R(t'')\big)\,\mathrm{d}t''\right]\mathrm{d}t'\,, \tag{162}$$

where $\Gamma_i\big(R(t)\big)$ is the rate of the decay via the ith channel. The total decay rate is defined as

$$\Gamma_{\mathrm{tot}} = \sum_i \Gamma_i = \Gamma_{\mathrm{sq},a} + \Gamma_{\mathrm{sq},b} + \Gamma_{1,b} + \Gamma_{1,a} + \Gamma_{ab}\,. \tag{163}$$

The total probability of the system being in any of the final states is equal to

$$\sum_i P_i(\varrho, t) = 1 - \exp\left[-\int_{-\infty}^{t} \Gamma_{\mathrm{tot}}(t')\,\mathrm{d}t'\right].$$

The sum of this probability and the probability (161) of finding the system in the initial state is equal to unity, as it should be.

The cross sections σ_A and σ_B of one-electron detachments from ions A^- and B^- are described as

$$\sigma_A = 2\pi\int_0^\infty \big(P_{\mathrm{sq},a}(\varrho) + P_{1,a}(\varrho)\big)\,\varrho\,\mathrm{d}\varrho\,,$$

$$\sigma_B = 2\pi\int_0^\infty \big(P_{\mathrm{sq},b}(\varrho) + P_{1,b}(\varrho)\big)\,\varrho\,\mathrm{d}\varrho\,, \tag{164}$$

$$P_0(\varrho) \equiv P_0(\varrho, t = +\infty)\,,$$

and the cross section σ_{AB} of two-electron detachment

$$\sigma_{AB} = 2\pi\int_0^\infty P_{ab}(\varrho)\,\varrho\,\mathrm{d}\varrho \tag{165}$$

has been calculated with the use of Coulomb trajectories $R(t)$, so that the behavior of cross sections near the thresholds has been reproduced correctly. The repulsion of the negative ions A^- and B^- controls these peculiarities.

The cross sections of the electron detachments in the collisions $H^- + H^-$, $H^- + Cs^-$ and $Cs^- + Cs^-$ are shown in Figs 13–15. The comparison with the measurement results is drawn in Fig. 13 for the example of the $H^- + H^-$ collision.

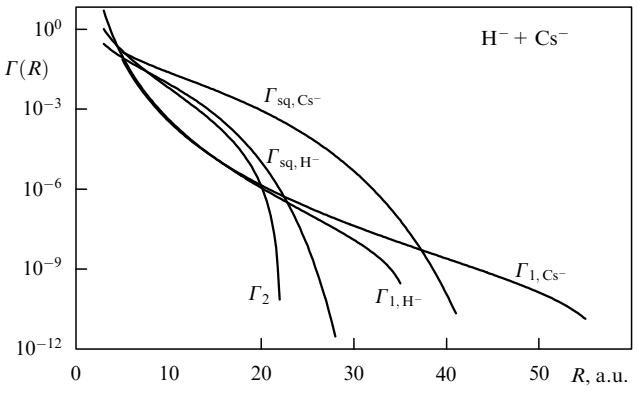

Figure 12. Partial decay rates as functions of internuclear distance R for the collision $H^- + Cs^-$: $\Gamma_{\mathrm{sq,H^-}}$ and $\Gamma_{\mathrm{sq,Cs^-}}$ are the rates of electron squeezing out from ions H^- and Cs^-, respectively, defined by formula (154); $\Gamma_{1,\mathrm{H^-}}$ and $\Gamma_{1,\mathrm{Cs^-}}$ — the rates of one-electron Auger decays with electron detachment from H^- and Cs^-, respectively, described by formulas (158) and (159), and Γ_2 — the rate of two-electron Auger decay, determined by formula (160).

3.2 High collision velocities. Dynamic detachment

At high collision velocities, the processes (A), (B), (AB) occur as a result of a direct transfer of part of the nuclear kinetic energy to weakly bound electrons. In paper [46], the system of equations for the coupling of the initial state with the continuum of states has been reduced in the dipole approximation to one integro-differential equation for the amplitude $a_0(t)$ of the initial state:

$$\frac{\mathrm{d}a_0}{\mathrm{d}t} = -S_A(t) - S_B(t) - S_{AB}(t)\,, \tag{166}$$

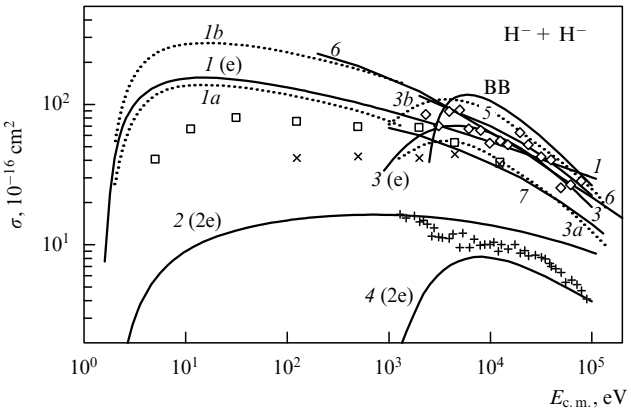

Figure 13. Cross sections of one- (e) and two- (2e) electron detachments in the $H^- + H^-$ collision as a function of the collision energy $E_{c.m.}$ in the center-of-mass system, obtained in the decay approach (curves *1* and *2*) and in the dynamic approach (curves *3* and *4*) [46]. Dotted curves: *1a* — electron squeezing out calculated for the collision $H^- + \bar{p}$ [46, 53], and *1b* — the double antiproton cross section *1a*; squares and inclined crosses — double cross section of electron detachment from H^- in collision with antiproton, obtained in classical Monte Carlo approach (two different calculations) [55, 56]; dotted curve *3a* — cross section of electron detachment by antiproton impact in dynamic approach [46]; dotted curve *3b* — double antiproton cross section; curve BB — double Bethe – Born cross section of one-electron detachment [46, 53]; diamonds and crosses — measured cross sections of one- and two-electron detachments, respectively [44, 45, 49]; curves *5* and *6* — theoretical estimates of the total cross section of a one-electron detachment with the use of the double antiproton cross section [49, 52], and curve *7* — total cross section of one-electron detachment calculated within the classical Monte Carlo approach [44].

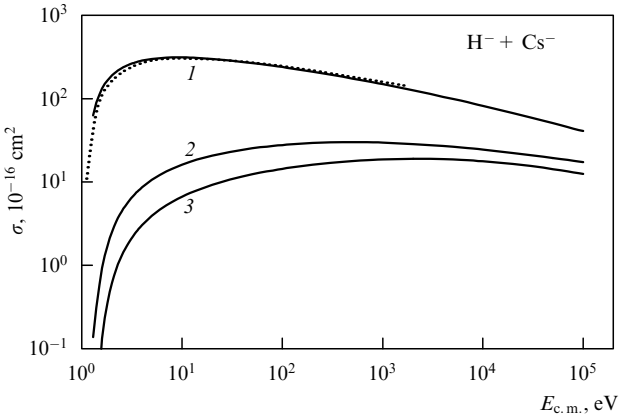

Figure 14. Cross sections of one- and two-electron detachments, calculated in the decay approach for the collision $H^- + Cs^-$: curves *1* and *2* — cross sections of one-electron detachment from the Cs^- and H^- ions, respectively; dotted curve — cross section of one-electron detachment by antiproton impact: $Cs^- + \bar{p} = Cs + \bar{p} + e$, and curve *3* — cross section of two-electron detachment $H^- + Cs^- = H + Cs + 2e$.

where the following notation is used:

$$S_{A,B}(t) = \int_{-\infty}^{t} a_0(t') \exp\left(i\varepsilon_{a,b}(t-t')\right) K_{A,B}(t,t')\,dt', \tag{167}$$

$$S_{AB}(t) = \int_{-\infty}^{t} a_0(t') \exp\left(i(\varepsilon_a+\varepsilon_b)(t-t')\right) K_{AB}(t,t')\,dt'. \tag{168}$$

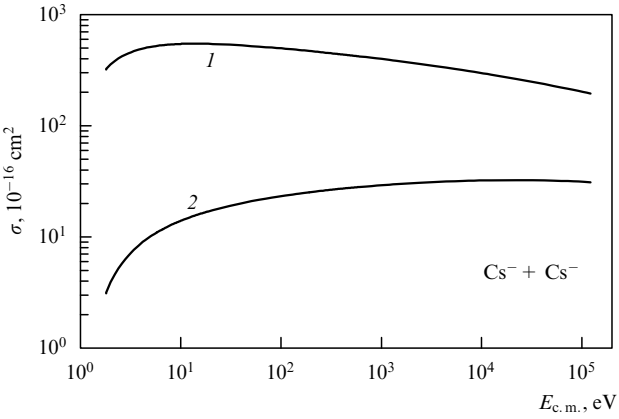

Figure 15. Cross sections of one- and two-electron detachments, calculated in the decay approach for the collision $Cs^- + Cs^-$: curve *1* — total cross section of one-electron detachments with the formation of $Cs + e + Cs^-$ or $Cs^- + Cs + e$ systems, and curve *2* — cross section of two-electron detachment $Cs^- + Cs^- = 2Cs + 2e$.

Equation (166) has been derived by the integration of the equation for the amplitude $a(\varepsilon, t)$ of the continuum state with energy ε with respect to time and the substitution of the result into the equation for the initial state amplitude $a_0(t)$ [46]. In the integro-differential equation (166), the kernels $K_{A,B}(t,t')$ are equal to

$$K_{A,B}(t,t') \equiv \int_0^{+\infty} V_{0\varepsilon}^{A,B}(t)\, V_{\varepsilon 0}^{A,B}(t') \exp\left(-i\varepsilon(t-t')\right) d\varepsilon, \tag{169}$$

$$K_{AB}(t,t') \equiv \int_0^{+\infty}\int_0^{+\infty} V_{0\varepsilon\varepsilon'}^{AB}(t)\, V_{\varepsilon\varepsilon' 0}^{AB}(t') \times \exp\left(-i(\varepsilon+\varepsilon')(t-t')\right) d\varepsilon\, d\varepsilon'. \tag{170}$$

Equation (166) has been solved numerically for every rectilinear trajectory of the atomic nuclei [46].

In the dipole approximation, the matrix elements $V^{A,B}(t)$ were calculated with the wave functions (155), (157) and kernels $K_{A,B,AB}(t,t')$ turned out to be equal to [46]

$$K_{A,B}(t,t') = \frac{4B_{a,b}^2}{3\pi|\varepsilon_{a,b}|} \frac{\cos\left(\varphi_R(t)-\varphi_R(t')\right)}{R^2(t)\,R^2(t')} F\left(|\varepsilon_{a,b}|(t-t')\right), \tag{171}$$

$$K_{AB}(t,t') = \frac{16B_a^2B_b^2}{3\pi^2|\varepsilon_a\varepsilon_b|} \frac{3\cos^2\left(\varphi_R(t)-\varphi_R(t')\right)-1}{R^3(t)\,R^3(t')} \times F(|\varepsilon_a|(t-t'))\,F(|\varepsilon_b|(t-t')), \tag{172}$$

where the spectral function is defined as

$$F(x) = \int_0^{\infty} \frac{y^{3/2}\exp(-ixy)}{(1+y)^4}\,dy. \tag{173}$$

The total cross sections of one- and two-electron detachments were calculated at high collision velocities with the use of rectilinear trajectories for the system $H^- + H^-$. These cross sections are shown in comparison with the measurement results in Fig. 13 [44, 45, 49]. For a symmetrical collision, the total cross section of one-electron detachment is equal to

the sum of the cross sections of the processes (A) and (B). This cross section calculated in the dynamic approximation is in good agreement with the results of experimental findings. We note that the experimental points are widely scattered.

The cross section of two-electron detachment, calculated in the dynamic approximation, is 15–20% smaller than the experimental one. This discrepancy is explained by the contribution of the process $H^- + H \to H + H + e$ to the experimental cross section [49]. This reaction, theoretically investigated for the first time in paper [61], takes place after the one-electron detachment and leads to the detachment of two electrons. Both the cross sections of dynamic detachments, calculated in work [46], exponentially decrease at adiabatically small collision energies $E_{c.m.} \leqslant 2-3$ keV.

In a collision of two negative ions, the electron detachment from one of the ions is in competition with the electron detachment from the other ion. Therefore, the probability of electron detachment, for example, from the ion H_a^- must be estimated by the product $P_a(1-P_b)$, where the $1-P_b$ is the probability of the ion H_b^- not being destroyed. The quantities $P_{a,b}$ are the probabilities of the ions $H_{a,b}^-$ being destroyed in the collision with an antiproton. Then the total probability of one-electron detachment is $P_a(1-P_b)+P_b(1-P_a)$. At large collision energies, the main contribution to the detachment cross section is made by collisions with large impact parameters, when the detachment probabilities are small: $P_{a,b} \ll 1$ and $1-P_{a,b} \sim 1$. In this case, the total probability of one-electron detachment is equal to the sum $P_a + P_b$ of probabilities of one-electron detachments and the total cross section comes out to $\sigma_a + \sigma_b$.

At the collision energies $E_{c.m.} \leqslant 10$ keV, the probabilities $P_{a,b}$ of one-electron detachments in collisions with antiproton are sharp functions of the impact parameter ϱ. At large ρ ($\varrho \gg 1$) they are close to zero, and over a narrow range $\delta\varrho$ they increase from zero to unity and remain close to unity at smaller ϱ. In this case the sum of probabilities is close to 2 ($P_a + P_b \approx 2$) over the main region of impact parameters ρ; therefore, for collisions of two negative ions neither probabilities nor cross sections can be added. The electron detachment from ion a is in competition with the electron detachment from ion b. As a result, in a collision of the like negative ions, the probability of electron detachment from one of the ions is two times smaller than that of the electron detachment in a collision with an antiproton. The total cross section of one-electron detachment is close in this case to the cross section of one-electron detachment in a collision with an antiproton, but not to the double cross section (see curve 1*b*, Fig. 13).

An analytical expression for the cross section of the electron detachment from H^- by electron impact was obtained in Ref. [53] using the Bethe–Born approximation. In order to compare this formula with the cross section of one-electron detachment in the collision $H^- + H^-$, we must consider the double Bethe–Born cross section, viz. the curve BB which is shown in Fig. 13. It can be seen from this figure that the Bethe–Born approximation overestimates a one-electron detachment cross section by two times in the peak region. Only at energies $E_{c.m.} \geqslant 100$ keV this approximation has an acceptable accuracy.

In a collision of two different ions $A^- + B^-$, the electron detachment from the ion with the smaller binding energy is more probable. The cross section of electron detachment from the ion Cs^- in the collision $H^- + Cs^-$ (curve *1* in Fig. 14) is larger than the cross section of electron detachment from H^- and is very close to the cross section of electron detachment from Cs^- by antiproton impact (the dotted curve in Fig. 14). At the same time, the cross section of ion H^- destruction (curve *2*) is about two times smaller than the cross section of electron detachment from one of the ions in the collision $H^- + H^-$ (see Fig. 13).

The cross sections of electron detachments in the collision $Cs^- + Cs^-$ are shown in Fig. 15. Comparing Figs 13 and 15 we may conclude that the total cross sections of one-electron detachment are inversely proportional to the square of the binding energies of negative ions. While the cross section of two-electron detachment very weakly increases when the binding energy of the colliding negative ions decreases.

4. Symmetrical collisions

In a symmetrical collision, the two-electron process of the ionization transfer is very interesting. In the collision $H^- + H^+$, the following processes take place:

$$H_a^- + H_b^+ \to H_a(1s) + H_b^*(n)\,, \tag{A1}$$

$$\to H_a(1s) + H_b^+ + e\,, \tag{A2}$$

$$\to H_a^+ + H_b(1s) + e\,. \tag{A3}$$

Process A1 presents the capture of a weakly bound electron discussed in the first section. The cross section of this process is the largest. Process A2 comprises electron detachment by proton impact. The cross section of this process is 2–4 times smaller than the cross section of electron capture. The third process A3 consists in ionization transfer. The cross section of this process is an order of magnitude smaller than the cross section of electron capture. In this section we discuss process A3.

Process A3 has been investigated experimentally [62] and has been interpreted as electron Auger decay from the excited repulsive molecular states which are responsible for the process of the associative ionization in the collisions $H^- + H^+$ and $H^* + H$ at low energies [63]. However, the process of associative ionization is effective at collision energies 0.01 eV– 5 eV, and at energies 10 eV–10 keV studied in Ref. [62] the cross section of associative ionization is very small. Therefore, another interpretation of process A3 has been proposed in paper [10]. Process A3 was considered there as a sequence of two processes: the detachment A2 with the sequential transition of the core 1*s*-electron from the atom H_a to the atom H_b. It is very well known that the cross section of the last transition, viz. the charge exchange process, is fairly large up to energies 25 keV [64].

In paper [10], the detachment channel in the system of close coupling equations has been described by an integro-differential equation similar to the description of electron detachments in a collision of two negative ions [46] (see previous section). The following system of equations has been solved numerically:

$$\frac{da_0}{dt} = -S_g(t) - S_u(t) - i\sum_n a_n(t)\, V_{0,n}(t)\, \exp\left(i\chi_{0n}(t)\right),$$

$$\cdots\cdots\cdots\cdots\cdots\cdots\cdots\cdots\cdots\cdots\cdots\cdots\cdots\cdots\cdots\cdots \tag{174}$$

$$\frac{da_n}{dt} = -i\, a_0(t)\, V_{n,0}(t)\, \exp\left(-i\chi_{0n}(t)\right).$$

where the notation was used as follows

$$\chi_{0n}(t) \equiv \left(\varepsilon_0 - E_n - \frac{v^2}{2}\right) t - J_{\mathrm{Coul}}(t)\,,$$

$$S_{g,u} = \int_{-\infty}^{t} a_0(t')\,\exp\left(\mathrm{i}\phi_{g,u}(t) - \mathrm{i}\phi_{g,u}(t')\right) K_{g,u}(t,t')\,\mathrm{d}t', \tag{175}$$

$$\phi_{g,u}(t) \equiv \varepsilon_0 t - \int_{-\infty}^{t} \left[E_{g,u}\big(R(t)\big) - E_{1s}\right] \mathrm{d}t' - J_{\mathrm{Coul}}(t)\,,$$

$$J_{\mathrm{Coul}}(t) \equiv \int_0^t \frac{1}{R(t')}\,\mathrm{d}t'\,.$$

The kernels $K_{g,u}$ in the dipole approximation are

$$K_{g,u}(t,t') = \alpha_{g,u}\,\frac{4N_0^2}{3\pi|\varepsilon_0|}\,\frac{\cos\left(\varphi_R(t) - \varphi_R(t')\right)}{R^2(t)\,R^2(t')}\,F\big(|\varepsilon_0|(t-t')\big), \tag{176}$$

where

$$\alpha_{g,u} = \left[1 \pm \frac{J(R)}{2}\right]^{1/2},$$

$$J(R) = \langle\psi_{1s,a}|\psi_{1s,b}\rangle = \left(1 + R + \frac{R^2}{3}\right)\exp(-R)\,.$$

Quantities $S_{g,u}$ and $K_{g,u}$ describe the detachment of the core $1s$-electron to the g and u states of the ion H_2^+ with energies $E_{g,u}(R)$.

After detachment of the weakly bound electron, the core $1s$-electron can be bound with the atom H_a or with the atom H_b. The probabilities $P_{a,b}$ of detachment of the weakly bound electron, accompanied by the core $1s$-electron transition to atoms $H_{a,b}$, are defined as

$$P_a(\varrho) = \mathrm{Re}\left\{\int_{-\infty}^{+\infty}\left[1 + \exp\left(-\mathrm{i}\int_t^{+\infty}\Delta_{gu}(t')\,\mathrm{d}t'\right)\right] \times \left[a_0^*(t)\,S_g(t) + a_0(t)\,S_u^*(t)\right]\mathrm{d}t\right\}, \tag{177}$$

$$P_b(\varrho) = \mathrm{Re}\left\{\int_{-\infty}^{+\infty}\left[1 - \exp\left(-\mathrm{i}\int_t^{+\infty}\Delta_{gu}(t')\,\mathrm{d}t'\right)\right] \times \left[a_0^*(t)\,S_g(t) + a_0(t)\,S_u^*(t)\right]\mathrm{d}t\right\}, \tag{178}$$

where $\Delta_{gu}\big(R(t)\big) \equiv E_g\big(R(t)\big) - E_u\big(R(t)\big)$.

The probability of process A3 is P_b. We see from the above expression that the probability of process A3 depends on the energy difference between the g and u states of the molecular ion H_2^+. This dependence is similar to the dependence of the resonance charge exchange probability in the collision $H_a(1s) + H_b^+ = H_a^+ + H_b(1s)$ [64]. If the energy difference of the g and u states is equal to zero ($E_g - E_u = 0$), then the probability of process A3 also comes to zero: $P_b = 0$.

The system of equations (174) has been solved numerically [10]. The energies $E_{g,u}(R)$ of the ion H_2^+ were taken from paper [65]. The cross section of process A1, derived in these calculations, is shown in Fig. 16 (curve *1*). This cross section has been previously measured [66–69] and calculated [70–82].

The cross section of process A3, calculated in paper [10] and shown in Fig. 17, is smaller than the experimental one.

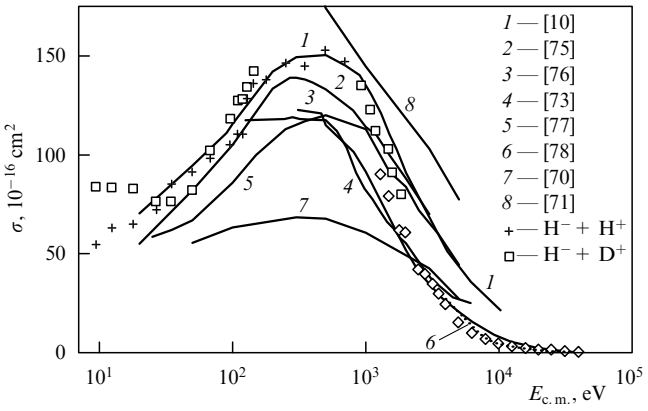

Figure 16. Cross section of mutual neutralization $H^- + H^+ = H(1s) + H^*(nlm)$ as a function of the collision energy in a center-of-mass system. Theory: curves *1–8*. Crosses and squares are the results of experimental investigations by merged beam method [66]: crosses for the $H^- + H^+$ collision and squares for the $H^- + D^+$ collision at the same collision velocity as that for $H^- + H^+$. Results of measurements carried out before the appearance of work [66] are not shown in the figure in view of their large uncertainties.

At large collision energies ($E_{\mathrm{c.m.}} > 1-2$ keV), the discrepancy is larger. This may be explained by the contribution of the process of the two-electron exchange $H_a^- + H_b^+ = H_a^+ + H_b^-$, which was neglected in the calculations [10]. The probability of this process is not relatively small [83]. Electron detachment from the ion H_b^- after this electron exchange leads to reaction A3. Notice that the theory of two-electron exchange [83] should be reconstructed for the case of collision $H^- + H^+$, because of the presence of one-electron resonances.

At energies smaller than 1 keV, the following sequence of transitions leading to reaction A3 should be taken into account [83]:

$$H_a^- + H_b^+ \to H_a(1s) + H_b^*(nlm) \to H_a^*(nlm) + H_b(1s)$$
$$\to H_a^+ + H_b^- \to H_a^+ + H_b(1s) + \mathrm{e}\,.$$

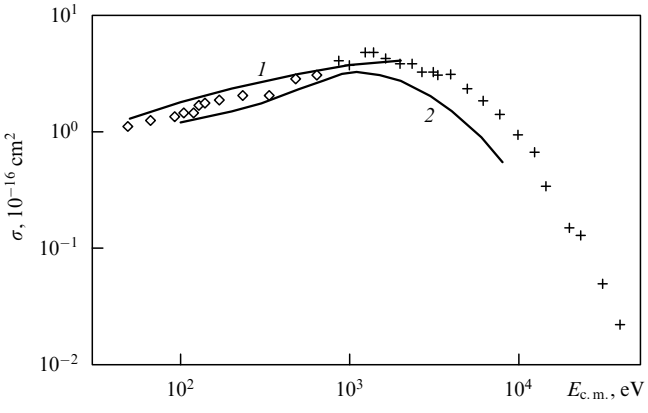

Figure 17. Cross section of the process $H_a^- + H_b^+ = H_a^+ + H_b(1s) + \mathrm{e}$ as a function of the collision energy in the center-of-mass system. Solid lines represent theoretical calculations: curve *1* — result of the autoionization model [62], and curve *2* — result of calculations [10]. Results of experimental studies [62]: diamonds — results of the group in Louvain-la-Neuve, and crosses — results of the Giessen group.

The first step in this sequence is the one-electron capture the probability of which is not small. The second step consists in the resonance exchange by excitation, which is effective at small collision velocities. The third step presents the reaction which is the reverse of the one-electron capture, and its probability is not small. As a result, the three first steps give rise to two-electron exchange. The subsequent electron detachment leads to reaction A3. This reaction sequence has not been investigated in details.

5. Conclusions

A detailed analysis of the exact expression for the Coulomb Green function is made in this review. This Green function was found by Hostler and Pratt as far back as 1963. Our analysis has permitted us to obtain new rich information about very well-known Coulomb systems: atomic hydrogen and hydrogen-like ions. In particular, sums of products of the Coulomb wave functions over degenerate manifolds, i.e. over orbital quantum numbers $\{l, m\}$ for a given principal quantum number n, have been obtained in a closed form. Such sums turned out to be equal to the quadratic forms of the wave functions with zero orbital quantum numbers ($l = m = 0$).

Wave functions of active covalent states of a Rydberg electron perturbed by a neutral atom, i.e. wave functions of the system $A^- + B^+$, are expressed through the sums discussed. The investigation of these sums shows that the Rydberg electron in such systems possesses a dipole moment. In the limit of large internuclear distances ($R \to \infty$), the Rydberg electron wave functions are transformed to Coulomb wave functions in parabolic coordinates, i.e. to the wave functions of Stark states of atomic hydrogen placed in a uniform electric field.

Adiabatic exchange matrix elements between ionic and covalent states of the $A^- + B^{Z+}$ system are expressed through analogous sums of Coulomb wave function products which depend on R. These sums do not come to nought at a finite value of R, and thus all crossings of ionic and covalent states are avoided crossings.

In this review we constructed the complete orthonormal basis of adiabatic wave functions for the $A^- + B^{Z+}$ system. The results are used for investigating collisions of negative ions having orbital momenta $L = 0$ and $L = 1$ with positive ions. The cross sections of electron captures in the collisions $H^- + H^+$ and $H^- + He^{++}$ were calculated and discussed.

Collisions of two negative ions were also investigated. The colliding system $A^- + B^-$ is a two-electron one. Therefore, the calculations were carried out for a doubled set of quantum states describing the one-electron detachments: $A + e + B^-$ and $A^- + B + e$.

This study was supported by the Council for Grants of the President of the Russian Federation and State Support for Leading Scientific Schools (grant No. 00-15-96526).

References

1. Hostler L, Pratt R H *Phys. Rev. Lett.* **10** 469 (1963)
2. Hostler L *J. Math. Phys.* **5** 591 (1964)
3. Komarov I V, Pogorelyĭ P A, Tibilov A S *Opt. Spektrosk.* **27** 198 (1969)
4. Presnyakov L P *Phys. Rev. A* **2** 1720 (1970)
5. Kereselidze T M, Chibisov M I *Zh. Eksp. Teor. Fiz.* **68** 12 (1975) [*Sov. Phys. JETP* **41** 5 (1975)]
6. Demkov Yu N, Ostrovskiĭ V N *Metod Potentsialov Nulevogo Radiusa v Atomnoĭ Fizike* (Zero-Range Potential Method in Atomic Physics) (Leningrad: Izd. LGU, 1975) [Translated into English as *Zero-Range Potentials and Their Applications* (New-York: Plenum Press, 1988)]
7. Landau L D, Lifshitz E M *Kvantovaya Mekhanika. Nerelyativistskaya Teoriya* (Quantum Mechanics: Non-Relativistic Theory) (Moscow: Nauka, 1974) [Translated into English (Oxford: Pergamon Press, 1977)]
8. Chibisov M I *Zh. Eksp. Teor. Fiz.* **120** 291 (2001) [*JETP* **93** 256 (2001)]
9. Chibisov M et al. *J. Phys. B* **30** 991 (1997)
10. Chibisov M I et al. *J. Phys. B* **31** 2795 (1998)
11. Chibisov M I et al. *Zh. Eksp. Teor. Fiz.* **117** 313 (2000) [*JETP* **90** 276 (2000)]
12. Chibisov M et al. *Phys. Rev. Lett.* **84** 451 (2000)
13. Cherkani M H, Brouillard F, Chibisov M I *J. Phys. B* **34** 49 (2001)
14. Khrebtukov D B, Fabrikant I I *Phys. Rev. A* **54** 2906 (1996)
15. Komarov I V, Ponomarev L I, Slavyanov S Yu *Sferoidal'nye i Kulonovskie Sferoidal'nye Funktsii* (Spheroidal and Coulomb Spheroidal Functions) (Moscow: Nauka, 1976)
16. Demkov Yu N, Komarov I V *Zh. Eksp. Teor. Fiz.* **50** 286 (1966) [*Sov. Phys. JETP* **23** 193 (1966)]
17. Eganova I A, Schirokov M I, Preprint OIYaI P4-5438 (Dubna: OIYaI, 1970); *Ann. Phys.* (Leipzig) **21** (5/6) (1968)
18. Davydov A S *Kvantovaya Mekhanika* (Quantum Mechanics) 2nd ed. (Moscow: Nauka, 1973) [Translated into English (Oxford: Pergamon Press, 1976)]
19. Fabrikant I I *J. Phys. B* **31** 2921 (1998)
20. Fabrikant I I, Chibisov M I *Phys. Rev. A* **61** 022718 (2000)
21. Fock V A "Atom vodoroda i neevklidova geometriya" ("Hydrogen atom and non-Euclidean geometry") *Izv. Akad. Nauk SSSR. Otd. Mat. Estestv. Nauk* **2** 169 (1935); "Zur theorie des wasserstoffatoms" *Z. Phys.* **98** 145 (1935)
22. Demkov Yu N, Komarov I V *Vestn. Leningrad. Univ.* **10** 18 (1965)
23. Beĭgman I L, Urnov A M, Shevel'ko V P *Zh. Eksp. Teor. Fiz.* **58** 1825 (1970) [*Sov. Phys. JETP* **31** 1015 (1970)]
24. Beigman I L, Urnov A M *J. Quant. Spectrosc. Radiat. Transf.* **14** 1009 (1974)
25. Vaĭnshteĭn L A, Sobel'man I I, Yukov E A *Vozbuzhdenie Atomov i Ushirenie Spektral'nykh Liniĭ* (Excitation of Atoms and Broadening of Spectral Lines) (Moscow: Nauka, 1979) [Translated into English (Berlin: Springer-Verlag, 1981)]
26. Lebedev V S, Beigman I L *Physics of Highly Excited Atoms and Ions* (Berlin: Springer-Verlag, 1998)
27. Greene C H, Dickinson A S, Sadeghpour H R *Phys. Rev. Lett.* **85** 2458 (2000)
28. Buchholz H *Die Konfluente Hypergeometrische Funktion* (Berlin: Springer-Verlag, 1953) [Translated into English: *The Confluent Hypergeometric Function with Special Emphasis on its Applications* (Berlin: Springer-Verlag, 1969)]
29. Slater L J *Confluent Hypergeometric Functions* (Cambridge: Cambridge Univ. Press, 1960)
30. Hughes J W B *Proc. Phys. Soc. London* **91** 810 (1967)
31. Berestetskiĭ V B, Lifshitz E M, Pitaevskiĭ L P *Relyativistskaya Kvantovaya Teoriya* (Relativistic Quantum Theory) Vol. 1 (Moscow: Nauka, 1968) [Translated into English (Oxford: Pergamon Press, 1971)]
32. Landau L D, Lifshitz E M *Kvantovaya Mekhanika. Nerelyativistskaya Teoriya* (Quantum Mechanics. Non-Relativistic Theory) (Moscow: OGIZ, 1948) [Translated into English (London: Pergamon Press, 1958)]
33. Smirnov B M *Dokl. Akad. Nauk SSSR* **161** 92 (1965)
34. Nikitin E E, Umanskiĭ S Ya *Neadiabaticheskie Perekhody pri Medlennykh Atomnykh Stolknoveniyakh* (Nonadiabatic Transitions at Slow Atomic Collisions) (Moscow: Atomizdat, 1979) [Translated into English as *Theory of Slow Atomic Collisions* (Berlin: Springer-Verlag, 1984)]
35. Terao M et al. *Europhys. Lett.* **1** 123 (1986)
36. Peart B, Bennett M A *J. Phys. B* **19** L321 (1986)
37. Cherkani M H et al. *J. Phys. B* **24** 209 (1991)
38. Cherkani M H et al. *J. Phys. B* **24** 2367 (1991)
39. Terao M et al. *Z. Phys. D* **7** 319 (1988)

40. Peart B, Wilkins P M *J. Phys. B* **19** L515 (1986)
41. Chenu J P et al., in *20th Intern. Conf. on the Physics of Electronic and Atomic Collisions* (*XX. ICPEAC*), *Vienna, Austria, 23 – 29 July, 1997* Abstracts of Contributed Papers, p. TU 187
42. Janev R K, Chibisov M I, Brouillard F *Phys. Scripta* **60** 403 (1999)
43. Radtsig A A, Smirnov B M *Zh. Eksp. Teor. Fiz.* **60** 521 (1971) [*Sov. Phys. JETP* **33** 249 (1971)]
44. Schulze R et al. *J. Phys. B* **24** L7 (1991)
45. Benner M et al., in *Tätigkeitsbericht. Strahlenzentrum des Justus-Liebig-Universität Giessen. Institut für Kernphysik* (Giessen: Strahlenzentrum, J. Liebig Universität, 1991) p. 46
46. Chibisov M I, Brouillard F, Cherkani M *Zh. Eksp. Teor. Fiz.* **119** 463 (2001) [*JETP* **92** 400 (2001)]
47. Chibisov M I, Yavlinskiĭ Yu N, Preprint IAE-5738/6 (Moscow: IAE, 1994)
48. Busic O, Grün N, Scheid W *J. Phys. B* **31** 2659 (1998)
49. Melchert F et al. *J. Phys. B* **28** 3299 (1995)
50. Uskov D B *Phys. Scripta T* **73** 133 (1997)
51. Presnyakov L P, Salzborn E, Tawara H, in *Atomic Physics with Heavy Ions* Ch. 16 (Springer Series on Atoms + Plasmas, 0177 – 6495, 26, Eds H F Beyer, V P Shevelko) (Berlin: Springer-Verlag, 1999) p. 349
52. Ostrovsky V N, Taulbjerg K *J. Phys. B* **29** 2573 (1996)
53. Smirnov B M, Chibisov M I *Zh. Eksp. Teor. Fiz.* **49** 841 (1965) [*Sov. Phys. JETP* **22** 585 (1966)]
54. Solov'ev E A *Zh. Eksp. Teor. Fiz.* **72** 2072 (1977) [*Sov. Phys. JETP* **45** 1089 (1977)]
55. Fiorentini G, Tripiccione R *Phys. Rev. A* **27** 737 (1983)
56. Cohen J S, Fiorentini G *Phys. Rev. A* **33** 1590 (1986)
57. Smirnov B M *Otritsatel'nye Iony* (Negative Ions) (Moscow: Atomizdat, 1978) [Translated into English (New York: McGraw-Hill, 1982)]
58. Radtsig A A, Smirnov B M *Parametry Atomov i Atomnykh Ionov. Spravochnik* (Parameters of Atoms and Atomic Ions. Reference Book) (Moscow: Energoatomizdat, 1986)
59. Chandrasekhar S *Astrophys. J.* **100** 176 (1944)
60. Zhdanov V P, Chibisov M I *Dokl. Akad. Nauk SSSR* **226** 1055 (1976)
61. Smirnov B M, Firsov O B *Zh. Eksp. Teor. Fiz.* **47** 232 (1964) [*Sov. Phys. JETP* **20** 156 (1965)]
62. Schön W et al. *Phys. Rev. Lett.* **59** 1565 (1987)
63. Urbain X et al. *J. Phys. B* **19** L273 (1986)
64. Firsov O B *Zh. Eksp. Teor. Fiz.* **21** 1001 (1951)
65. Bates D R, Ledsham K, Stewart A L *Philos. Trans. R. Soc. London Ser. A* **246** 215 (1953)
66. Szücs S et al. *J. Phys. B* **17** 1613 (1984)
67. Peart B, Bennett M A, Dolder K *J. Phys. B* **18** L439 (1985)
68. Peart B, Hayton D A *J. Phys. B* **25** 5109 (1992)
69. Schön W et al. *J. Phys. B* **20** L759 (1987)
70. Bates D R, Lewis J T *Proc. Phys. Soc. London Ser. A* **68** 173 (1955)
71. Dalgarno A, Victor G A, Blanchard P, Air Force Cambridge Research Laboratory Report No. 71-0342 (Cambridge, 1971)
72. Sidis V, Kubach C, Fussen D *Phys. Rev. Lett.* **47** 1280 (1981)
73. Sidis V, Kubach C, Fussen D *Phys. Rev. A* **27** 2431 (1983)
74. Fussen D, Kubach C *J. Phys. B* **19** L31 (1986)
75. Ermolaev A M *J. Phys. B* **21** 81 (1988)
76. Shingal R, Bransden B H, Flower D R *J. Phys. B* **18** 2485 (1985)
77. Errea L F et al. *Nucl. Instrum. Meth. B* **98** 335 (1995); *Phys. Rev. A* **54** 967 (1996)
78. Borondo F, Macias A, Riera A *Phys. Rev. Lett.* **46** 420 (1981); *Chem. Phys.* **81** 303 (1983); *Chem. Phys. Lett.* **100** 63 (1983)
79. Gayet R, Janev R K, Salin A *J. Phys. B* **6** 993 (1973)
80. Peart B, Grey R, Dolder K T *J. Phys. B* **9** 3047 (1976)
81. Bell K L, Kingston A E, Madden P J *J. Phys. B* **11** 3977 (1978)
82. Fussen D, Claeys W *J. Phys. B* **17** L89 (1984)
83. Chibisov M I *Zh. Eksp. Teor. Fiz.* **70** 1687 (1976); **75** 46 (1978) [*Sov. Phys. JETP* **43** 960 (1976); **48** 25 (1978)]
84. Gradshteĭn I S, Ryzhik I M *Tablitsy Integralov, Summ, Ryadov i Proizvedeniĭ* (Tables of Integrals, Sums, Series, and Products) 4th ed. (Moscow: Fizmatgiz, 1962) [Translated into English: Gradshteyn I S, Ryzhik I M *Table of Integrals, Series, and Products* (New York: Academic Press, 1979)]